NASA Goddard Space Flight Center
Greenbelt, Maryland 20771

NASA/TM-1998-208605

NASA Ocean Altimeter Pathfinder Project

Report 1: Data Processing Handbook

Contributors

C. J. Koblinsky

NASA/Goddard Space Flight Center

Brian D. Beckley

Richard D. Ray

Yan-Ming Wang

Lucia Tsaoussi

Anita Brenner

Ron Williamson

Raytheon STX Corporation

Version 1.0   *April 1, 1998*

Table of Contents

TABLES

FIGURES

1. Introduction

The NOAA/NASA Pathfinder program was created by the Earth Observing System (EOS) Program Office to determine how existing satellite-based data sets can be processed and used to study global change. The data sets are designed to be long time-series data processed with stable calibration and community consensus algorithms to better assist the research community.

The Ocean Altimeter Pathfinder Project involves the reprocessing of all altimeter observations with a consistent set of improved algorithms, based on the results from TOPEX/POSEIDON (T/P), into easy-to-use data sets for the oceanographic community for climate research. This report describes the processing schemes used to produce a consistent data set and two of the products derived from these data. Other reports have been produced that: a) describe the validation of these data sets against tide gauge measurements and b) evaluate the statistical properties of the data that are relevant to climate change.

The use of satellite altimetry for earth observations was proposed in the early 1960s ("Williamstown Report," MIT, 1970). The first successful space based radar altimeter experiment was flown on SkyLab in 1974 (McGoogan, et al., 1974). The first successful satellite radar altimeter was flown aboard the Geos-3 spacecraft between 1975 and 1978 (The Geos-3 Project, 1979). While a useful data set was collected from this mission for geophysical studies, the noise in the radar measurement and incomplete global coverage precluded it from inclusion in the Ocean Altimeter Pathfinder program. This program initiated its analysis with the Seasat mission, which was the first satellite radar altimeter flown for oceanography (Seasat, 1982). This mission was followed by the U.S. Navy's Geosat satellite in 1985 to 1989 (Geosat, 1987, 1990a, 1990b). The European Space Agency's ERS-1 spacecraft was flown from 1991 to 1996 (ERS-1 System, 1992). ERS-1 was followed by the joint U.S. and French T/P mission from 1992 to the present (TOPEX/Poseidon, 1994, 1995) and ESA's ERS-2 spacecraft in 1996 (ERS-2 Spacecraft, 1995). Table 1 summarizes the dates of these missions, the data coverage, and the length of time for which a Pathfinder data set has been constructed.

The second section of this report describes the algorithms that are used to process these data sets into a consistent cross mission data set for climate studies. The third and fourth sections describe two data products that have been produced from the corrected data. In section 3, a collinear product is described that is, essentially, time series of sea surface height along the track of the spacecraft. In these data only minimal interpolation and smoothing have been done to the measurement. In section 4, a grid data set is described where monthly anomalies relative to an annual reference surface have been created from all missions to provide a decade long data set of sea level anomalies.

The validation of the data sets are described in Pathfinder Report #2 and a statistical description of sea surface topography based on these data are described in Report #3.

Table 1: Satellite altimeter missions and data sets between 1975 and 2000.

	Mission Dates	Geophysical Data Record Dates	Pathfinder Data Dates
Seasat	6/26/78 – 10/10/78		
17 day near repeat		7/7/78 – 9/10/78	7/78 – 9/78
3 day repeat		9/11/78 – 10/10/78	9//78 – 10/78
Geosat	3/12/85 – 12/31/89		
Primary Mission		3/30/85 – 9/30/86	4/85 – 9/86
Exact Repeat Mission		11/8/86 – 12/31/89	11/8/86 – 8/22/89
ERS-1	7/17/91 – 2/6/96		
Phase A – 3 day commissioning phase	7/31/91 – 12/20/91	7/31/91 – 12/20/91	Not processed
Phase B – 3 day	12/28/91 – 3/30/92	12/28/91 – 3/30/92	12/28/91 – 3/30/92
Phase C – 35 day	4/14/92 – 12/20/93	4/14/92 – 12/20/93	4/14/92 – 12/20/93
Phase D – 3 day	12/23/93 – 4/10/94	12/23/93 – 4/10/94	12/23/93 – 4/10/94
Phase E – 168 day	4/10/94 – 9/27/94	4/10/94 – 9/27/94	4/10/94 – 9/27/94
Phase F - 168 day	9/27/94 – 3/21/95	9/27/94 – 3/21/95	9/27/94 – 3/21/95
Phase G – 35 day	3/21/95 – 6/2/96	3/21/95 – 6/2/96	3/21/95 – 6/2/96
TOPEX/POSEIDON	8/10/92 - Present	9/23/92 - Present	9/23/92 – Present
ERS-2 - 35 Day	4/20/95 - Present	4/21/95 - Present	4/21/95 – Present

The satellite altimeter measurement of surface height is observed by merging two complicated measurements, the radial position of the space-based ranging instrument relative to the center of the planet, and the round-trip travel time of a radar or light pulse sent from the spacecraft (see Figure 1). To transform satellite altimeter range and orbit measurements into accurate sea-surface elevation data, a variety of models, algorithms, and corrections need to be adopted and applied. These include the determination of the satellite position within a consistent geodetic reference frame, the correction for atmospheric range refraction and radar ranging corrections, and the removal of unwanted geophysical effects, such as tides and atmospheric loading. Most of the adopted PATHFINDER corrections and algorithms are consistent across satellite missions, but some are specific to an individual mission. Table 2 provides a summary of these many parameters for the satellites listed in Table 1. In this section, these algorithms are described.

• *Figure 1   A schematic of the satellite altimeter measurement of sea surface topography.*

8
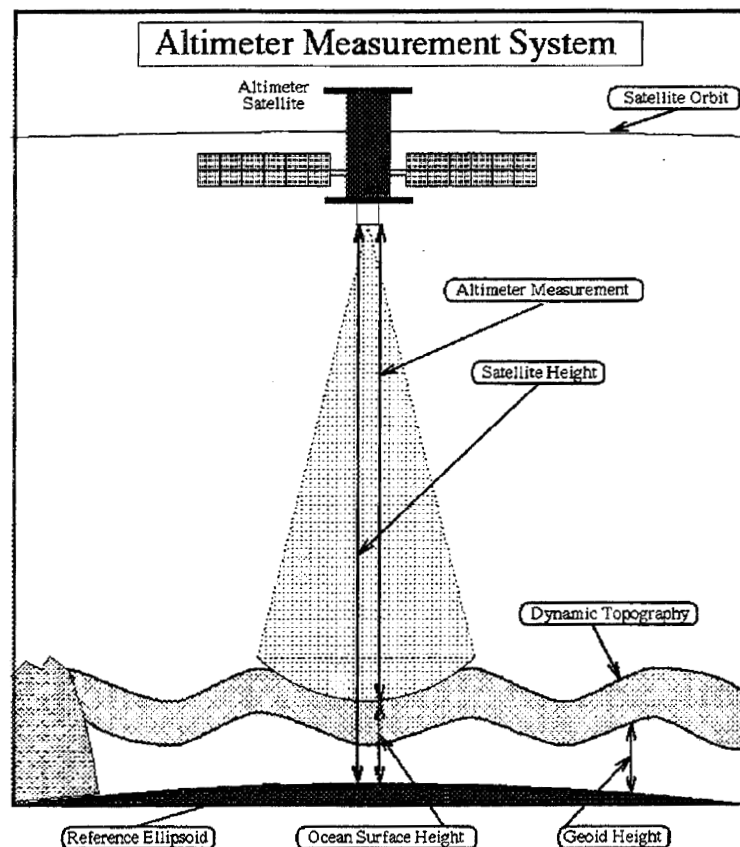
• *Table 2 Summary of Algorithms used to process satellite altimeter data.*

Satellite -> Algorithm I	TOPEX	POSEIDON	ERS-1	Geosat	Seasat
II.A. Position					
Orbit	T/P POD 2 JGM-3	T/P POD 2 JGM-3	Delft DGM-E04	Goddard JGM-3	Goddard JGM-3
Geodetic ref	ITRF	ITRF	ITRF	ITRF	ITRF
Ref Ellipsoid	T/P	T/P	T/P	T/P	T/P
II.B. Instrument					
Sea State Bias	Walsh	Gaspar BM4	Gaspar BM1	Gaspar BM3	Gaspar
Retracking	None	CNES	ESTeC	Goddard	Goddard
Calibration	Range, Oscillator, Sigma 0 Drifts	CNES	Range bias	Cal mode and oscillator drifts, Range bias	Range bias
II.C. Atmospheric Refraction					
Dry Atmos.	Saastamoinen w/ ECMWF	Saastamoinen w/ ECMWF	Saastamoinen w/ ECMWF	Saastamoinen w/ ECMWF	Saastamoinen w/ FNOC
Wet Atmos.	Measured	Measured	Measured	NCEP Reanalysis	Measured
Ionosphere	Measured	DORIS	IRI95	IRI95	IRI95
II.B. Geophysical Models					
Earth Tide	Modified Wahr (1981)	Modified Wahr (1981)	Modified Wahr (1981)	Modified Wahr (1981)	Modified Wahr (1981)
Ocean Tide	Schrama & Ray (1994) SR960104	Schrama and Ray (1994) SR960104	Schrama and Ray (1994) SR960104	Schrama and Ray (1994) SR960104	Schrama and Ray (1994) SR960104
Load Tide	SR960104	SR960104	SR960104	SR960104	SR960104
Pole Tide	IERS	IERS	IERS	IERS	IERS
Geoid Gradient	UTCSR Mean Surface	UTCSR Mean Surface	UTCSR Mean Surface	UTCSR Mean Surface	UTCSR Mean Surface
Atmos Load	IB w/ECMWF	IB w/ECMWF	IB w/ECMWF	IB w/ECMWF	IB w/FNOC

2.1. Orbits

2.1.1. TOPEX/POSEIDON Precise Ephemerides

The precise satellite ephemerides for T/P are identical to those used in the second generation T/P Geophysical Data Records (GDRs) produced by the TOPEX Project Office. These ephemerides are of unprecedented accuracy, and they are, in large part, responsible for the enhanced accuracy of T/P over any other historical or present-day satellite-altimeter mission. The ephemerides are produced by the Space Geodesy Branch at NASA Goddard Space Flight Center (GSFC). They are computed for nominal 10-day arc segments, corresponding to the ground-track repeat period of the satellite. They are based on a combination of laser and doppler tracking data and on force models derived from the JGM-3 earth gravity model, a T/P-based ocean-tide model, and a `box-wing' satellite model for drag and radiation forces. The first-generation of these orbits are described by Nerem et al. (1993) and Tapley et al. (1994). The present version of the orbits is described by Marshall et al. (1995), who examine in detail the error budget and present evidence for a radial orbit accuracy of about 2 to 3 cm rms.

The Joint Gravity Model 3 (JGM-3) is an update to the JGM-1 and JGM-2 models developed at GSFC and the University of Texas and described by Nerem et al. (1994). The JGM-1 model was developed before the launch of T/P. It was the result of a multi-year effort to improve the earth's gravity model by a new inversion of tracking data on over 30 satellites, altimeter data from Seasat and Geosat, and direct gravity measurements on the earth's surface (land and marine gravimetry). The JGM-2 model was a `tuning' of JGM-1 after the launch of T/P by inclusion of 150 days of T/P tracking observations. The JGM-2 model was used for computing the first-generation orbits on the original T/P GDRs. The JGM-3 model represents a further tuning of JGM-1 by inclusion of more tracking data on T/P, and especially the inclusion of about 40 days of GPS tracking. The JGM-3 model is described in detail by Tapley et al. (1996).

The tidal perturbations on the satellite are deduced from a new ocean-tide model developed by Ray et al. (1994) that was produced primarily from T/P altimetry. Poleward of T/P's maximum 66° latitude, the model was supplemented by Schwiderski's older hydrodynamic model. Spherical harmonics through degree and order 15 are used from this ocean model to compute satellite perturbations, except for the resonant terms (degree-2, order-2 semidiurnals, degree-2, order-1 diurnals) which are taken from the tracking-based GEM-T3S model of Lerch et al. (1992). In addition to the ocean tide, of course, the earth tide also produces satellite perturbations. The earth model developed by Wahr (1981) is used. Any error in the earth tide will be absorbed, and hence adequately compensated for, by the GEM-T3 ocean resonance terms.

The box-wing model which is used for modeling forces arising from atmospheric drag, solar and earth radiation, and spacecraft radiation has been described in detail by Marshall and Luthcke (1994a; 1994b).

Four different tracking systems are available on T/P: a) French Doppler Orbitography and Radiopositioning Integrated by Satellite (DORIS) system; b)

Satellite Laser Ranging (SLR); c) satellite-satellite tracking via the Tracking and Data Relay Satellite System (TDRSS), and d) Global Positioning System (GPS). For these computed orbits, only the two `operational' tracking methods (DORIS and SLR) are used. (The TDRSS and GPS data have been used by GSFC and other groups for orbital accuracy assessments and for other studies.) During the force-model integration and the fitting to the tracking data, one-per-revolution acceleration adjustments are also included to handle any remaining modeling errors; the theory for this adjustment is described by Colombo (1986) and Cretaux et al. (1994). Many other details concerning these orbits, including critical details concerning the geodetic reference frame and tracking station positioning, are described in the references mentioned above.

Analysis of collinear sea surface height residuals reveals dominant mesoscale oceanographic features as well as providing a statistical assessment of orbit models, geophysical and environmental height corrections. No adjustments were performed to correct for systematic orbit errors for the maps shown in figures 2-4.

• *Figure 2 T/P Sea Surface Height Variability 1993-1995.*
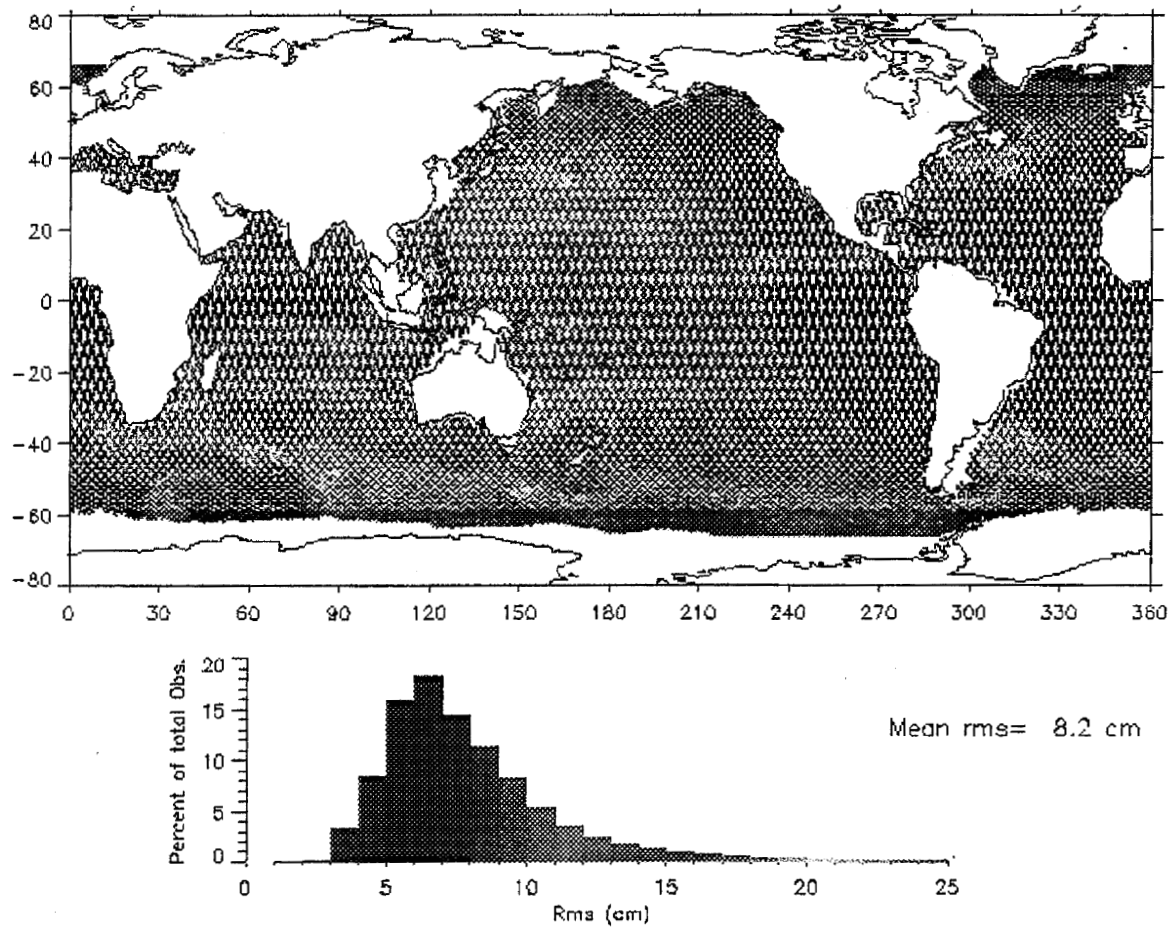
2.1.2. ERS-1 Precise Ephemerides Version 2.0

The precise satellite ephemerides for the ERS-1 mission (Phases B to G) have been computed at the Delft Institute for Earth-oriented Space Research (DEOS), Delft University of Technology. The computations used the DGM-E04 gravity field model (Scharroo et al., 1997). The DGM-E04 is a tuning of the JGM-3 model (Tapley et al., 1996) especially for handling ERS-1 and ERS-2. The tracking data on ERS-1 consists of satellite laser ranging only.

The radial orbit accuracy for the Phase C orbits (eighteen 35-day repeat cycles) is approximately 6-8 cm rms. The average ERS-1 altimeter crossover residual rms is about 10 cm for 1-sigma, including an estimate for geographically correlated orbit errors due to gravity.

- *Figure 3 ERS-1 Phase C Sea Surface Height Variability.*

Mean rms= 9.0 cm
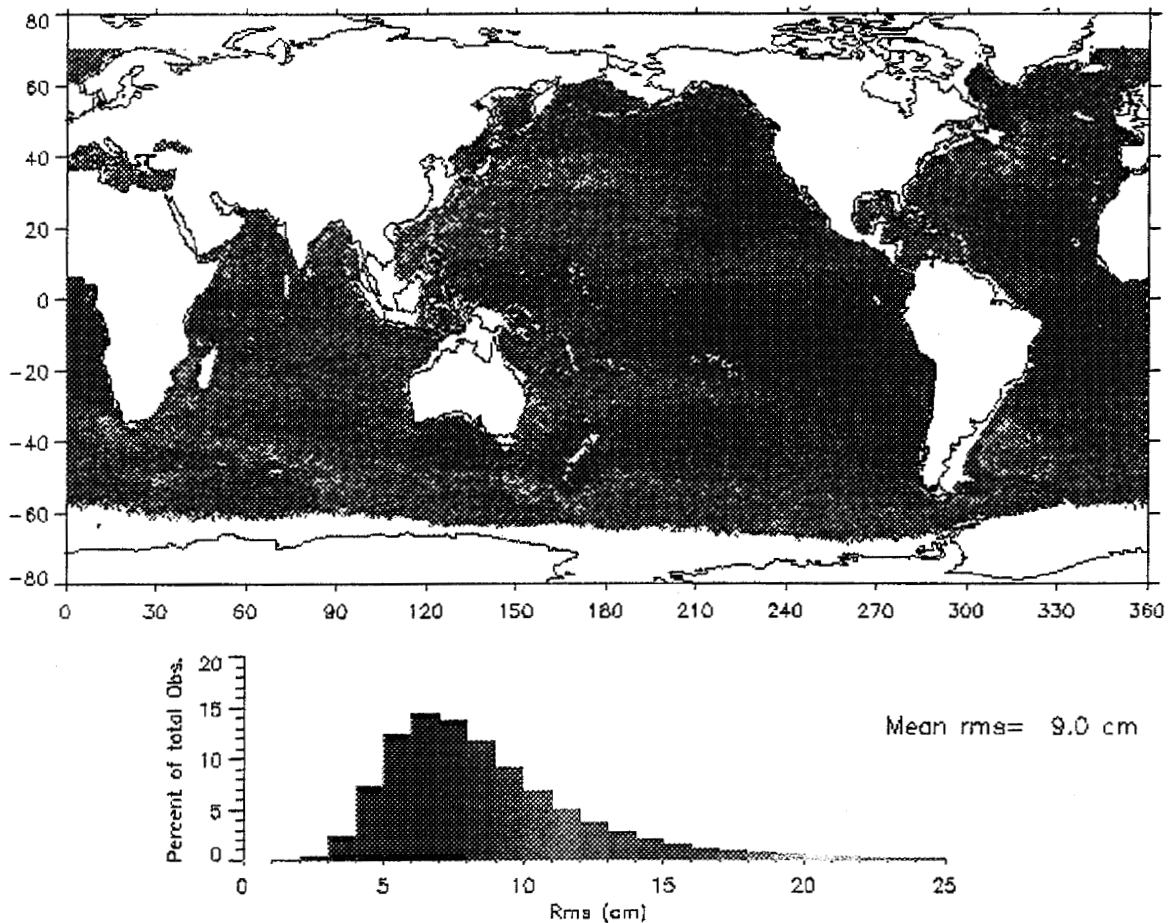
2.1.3. Geosat Precise Ephemerides

The satellite ephemerides for Geosat were computed at GSFC (Williamson and Nerem, 1994). They are based on TRANET Doppler tracking data collected at

some 45 ground stations and on force models that include the JGM-3 Earth gravity model and a T/P-based ocean-tide model.

The tidal forces on the satellite are computed using the same ocean-tide model that was used in the T/P ephemerides (Ray et al., 1994). Spherical harmonics through degree and order 15 are used from this ocean model to compute satellite forces, except for the resonant terms (degree-2, order-2 semidiurnals, degree-2, order-1 diurnals) which are taken from the tracking-based GEM-T3S ocean-tide solution of Lerch et al. (1992).

• *Figure 4 Geosat Sea Surface Height Variability During the First Year of the Exact Repeat Mission.*
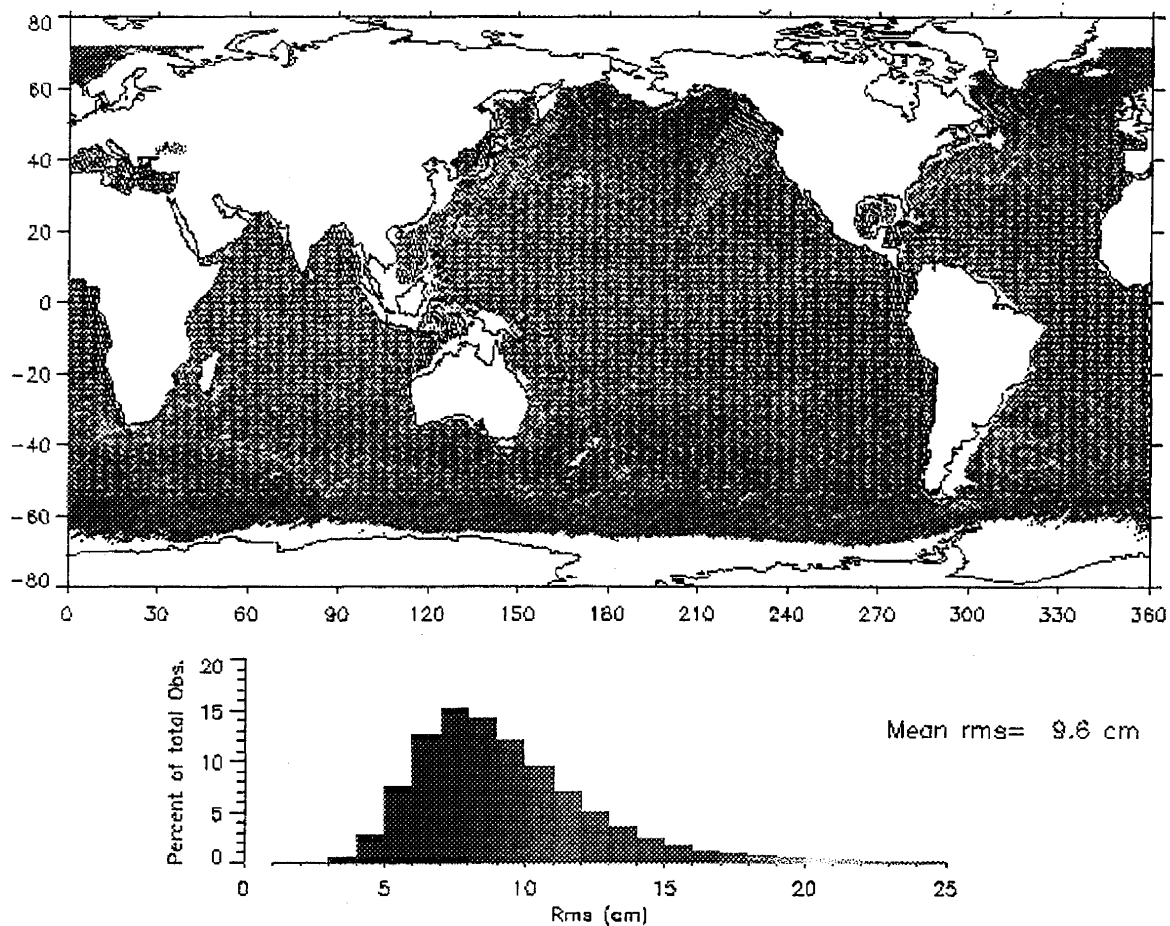
2.1.4. Seasat Precise Ephemerides

Precise Seasat ephemerides based upon JGM-3 were also computed at GSFC. These orbits are based upon TRANET Doppler, Unified S-Band (USB), and satellite laser ranging data. The force modeling is as was described above for Geosat. The USB tracking station coordinates required for Seasat were not available from the JGM-2/3 solution, so these were recovered from analyses of

the Seasat tracking data, holding fixed the TRANET sites and most of the lasers. Fifteen USB site locations were adjusted, as were the three SAO laser sites at Arequipa, Mt Hopkins, and Natal. These SAO site locations were adjusted because, with the current orbital accuracies, laser data biases in the early part of the Seasat Mission were both more detectable and separable from the site locations.

The predominant relevance of the USB tracking is that, in the early part of July 1978, TRANET tracking is not available, and there is only very sparse laser tracking. Thus the recovery of USB coordinates enables the computation of these earlier orbits in the same reference frame as the latter orbits.

It should be noted that the USB data do have some associated unmodeled ionosphere errors and so the earlier orbits are expected to be somewhat less accurate than in the latter period.

2.2. Reference Frames

2.2.1. Geodetic Reference Frame

The geodetic reference frame, which is consistently used in the PATHFINDER reprocessing for all altimeter satellite data, is the International Terrestrial Reference Frame (ITRF). The ITRF definition and other current modeling recommendations of the International Earth Rotation Service are documented in their "IERS Conventions," (McCarthy, 1996).

In the context of reference systems and station positioning, it is interesting to note the special case of Geosat, which was tracked only by the TRANET Doppler system. Were it not for the Seasat mission, which employed both TRANET and SLR tracking, it would be very difficult to adjust Geosat TRANET tracking sites into the ITRF. Thus, Seasat is important not only for its altimetry, but also for its tracking data. Appropriate use of those data allows Geosat to be tied into the same geodetic reference system as T/P. Work is still in progress to strengthen this tie. A consistent geodetic reference frame is crucial to climate-related studies.

2.2.2. Reference Ellipsoid

The reference ellipsoid used for all Pathfinder altimeter products is consistent with the official T/P GDRs.

Table 3 Reference Ellipsoid Parameters.

Term	Value
Equatorial radius	6378136.3 m
Flattening	1/298.257
Potential	62636858.702 m^2/s^2
G Me	398600.4415 km^3/s^2

14

2.3.   Instrument Corrections

2.3.1.   Sea State Bias

The sea-state bias correction compensates for the bias of the altimeter range measurement toward the troughs of ocean waves. This bias is thought to arise from three interrelated effects: a tracker bias, a skewness bias, and an electromagnetic (EM) bias. The correction for this bias is dependent on some percentage, usually some variable percentage, of the significant wave heights.

2.3.1.1.TOPEX

For the NASA TOPEX altimeter we adopted the EM-bias model devised by Ed Walsh (T/P GDR Handbook, Callahan 1993) with no additional tracker bias. This model is parametrically equivalent to the one used on the original TOPEX GDRs, but the values themselves are different for the following reasons:

1. Backscatter coefficients (σ_0) have been adjusted for the calibration results of Callahan, Hancock, and Hayne (1994; this reference gives adjustments only through cycle 40; other cycles are personal communications).
2. Wind-speed algorithm implementation, see below.

The present algorithm is thus

$$Eq.\ 1:\quad T/P\ SSB = H_{sw}\ (0.0029 + 0.0038\ U - 0.00015\ U^2)$$

where, H_{sw} is the altimeter observed significant wave height in meters, U is the altimeter observed 10-m wind speed in meters/second inferred from the adjusted σ_0 by using the modified Chelton-Wentz (MCW) algorithm with an additional -0.63 dB offset. Witter and Chelton (1991) describe the MCW algorithm. Callahan, Morris, and Hsiao (1994) describe the offset. The T/P SSB is in meters.

2.3.1.2.POSEIDON

The Poseidon altimeter is the CNES altimeter aboard the T/P satellite, nominally it is turned on for every 10th cycle of T/P observations. For this altimeter we adopted an updated version of the algorithm published by Gaspar et al. (1994), `BM4'. (Update coefficients from P. Gaspar, personal communication.) This is a four-coefficient model, determined by an empirical study of Poseidon crossover residuals. The model uses as independent variables the observed significant wave height H_{sw} and the inferred wind speed U, the latter being deduced from the backscatter cross-section coefficient, σ_0, by use of the MCW algorithm. The algorithm is

$$\bullet\ Eq.\ 2\ POSEIDON\ SSB = H_{sw}\ (0.047 + 0.0023\ U - 0.000112\ U^2 - 0.001\ H_{sw})$$

Where, H_{sw} is in meters, U in meters/second, and POSEIDON SSB is in meters.

2.3.1.3. ERS-1

For the ERS-1 altimeter we adopted a simple sea-state bias correction using a constant percentage of significant wave height. This percentage is taken as 5.5%, following an unpublished study of ERS-1 crossover data by Philippe Gaspar. The fact that the percentage (5.5) is much higher than the nominal 2% used for some altimeters indicates a significant tracker bias, similar though not quite as large as that seen on Seasat. Gaspar found little statistically significant dependence on wind speed, although this dependence has been established for other altimeters and in ground-based measurements.

In summary the correction used in this Pathfinder product is

- *Eq. 3   ERS-1 SSB $= 0.055\, H_{sw}$*

Where, H_{sw} is in meters, and ERS-1 SSB is in meters.

2.3.1.4. Geosat

For correcting the Geosat altimeter for the sea-state bias, we have relied on the study by Gaspar and colleagues (1996, Pathfinder Report #4) who recommend:

- *Eq. 4   Geosat SSB $= H_{sw}\, (-0.025 - 0.00145\, U + 0.00020\, H_{sw}\, U)$*

Where, H_{sw} is in meters, U is the inferred wind speed in meters/second, and Geosat SSB is in meters. The wind speed U is deduced from the backscatter coefficient (σ_0) using the Freilich and Challenor (1994) Rayleigh-based relation. This gives the wind speed at 19.5 m. The speed is divided by 1.057 to obtain a 10-m neutral stability wind speed.

2.3.1.5. Seasat

Prior estimates of the sea state bias for SEASAT ranged between 6-7% of the significant wave height (Born et al. 1982, Douglas and Agreen, 1983). After retracking the ocean returns, our preliminary estimate of the sea state bias is 2.7% of the significant wave height (P. Gaspar, personal communication, 1997). An empirical study of the SEASAT crossover residuals is currently being performed by Phillipe Gaspar to provide a formal estimate of the sea state bias.

2.3.2. Range Retracking

2.3.2.1. TOPEX – Carried out by Ernesto Rodridquez of JPL but we have not applied these to the data set

2.3.2.2. POSEIDON – Carried out and applied to GDR by CNES

2.3.2.3. ERS-1 – Carried out and applied to GDR by CERSAT

2.3.2.4. Geosat and Seasat

The Ice Altimetry Group of NASA/Goddard Space Flight Center (GSFC) and Hughes STX have developed algorithms for retracking polar ice altimetry returns to account for the inability of the on-board tracker to follow the topography of the ice sheets. The Seasat and Geosat altimeter data returns from the sensor data records (SDR's) were retracked employing the GSFC Version 2 retracker. Details of the retracking concepts and the Version 2 algorithm are described below and can also be accessed at:
http://crevasse.stx.com/ia_home/retrack/gsfcretrackdoc.960725.html

GSFC Retracking Concept

The GSFC algorithms are based on the concept that the return can be represented mathematically using a function described by Parsons 1979 over the Gaussian ocean surface. Typical ocean returns are shown in Figure 5. The measurement corresponding to the midpoint of the ramp gives the median elevation within the pulse-limited footprint. The on-board tracker tries to align the return so the midpoint of the ramp occurs at the tracking gate. For the ocean surfaces this works very well as indicated by the retracking correction varying from 3-6 cm. The longer vertical line indicates the position of the on-board tracking gate, whereas the short vertical line indicates the midpoint of the ramp, where the tracker should have been tracking to, as determined by the retracking process.

• Figure 5   Typical Ocean Waveforms over Antarctic Ocean from Geosat.
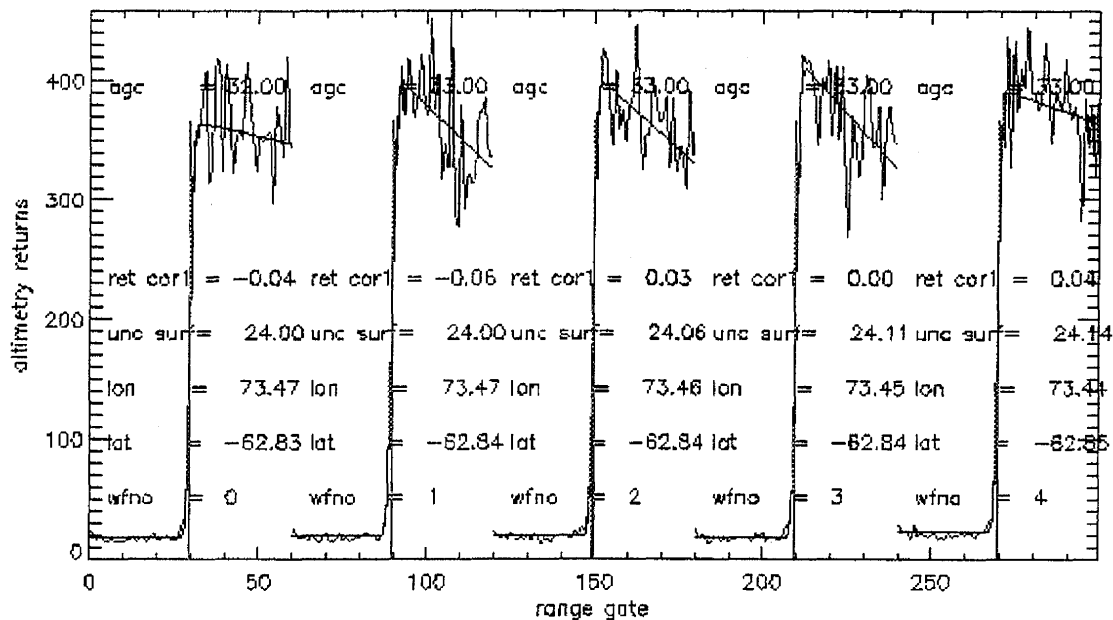
An iterative Bayesian least squares procedure is used to fit the digitized waveform to the appropriate function. For the single ramp return, a modified version of the ocean return function is used where an additional slope parameter is added after the ramp.

$$y = \beta_1 + \beta_2(1 + \beta_5 Q)P\left(\frac{t - \beta_3}{\beta_4}\right)$$

where:

$$Q = \begin{cases} 0 & \text{for } t < \beta_3 + .5\beta_4 \\ t - (\beta_3 + .5\beta_4) & \text{for } t \geq \beta_3 + .5\beta_4 \end{cases}$$

$$P(z) = \int_{-\infty}^{z} \frac{1}{\sqrt{2\pi}} e^{(-q^2/2)} dq$$

The mid-point of the ramp, Beta(3), is chosen as the correct range point, and the retracking correction is the displacement of that mid-point from the tracker gate. The linear trailing-edge of the function simulates the slowly decreasing return from a diffuse reflecting surface as the pulse expands over the beam-limited footprint. A nine-parameter function is used to simulate the double-peaked returns.

$$y = \beta_1 + \beta_2(1 + \beta_9 Q_1)P\left(\frac{t - \beta_3}{\beta_4}\right) + \beta_5(1 + \beta_8 Q_2)P\left(\frac{t - \beta_6}{\beta_7}\right)$$

where:

$$Q_1 = \begin{cases} 0 & \text{for } t < \beta_3 + .5\beta_4 \\ t - (\beta_3 + .5\beta_4) & \text{for } t \geq \beta_3 + .5\beta_4 \end{cases}$$

$$Q_2 = \begin{cases} 0 & \text{for } t < \beta_6 + .5\beta_7 \\ t - (\beta_6 + .5\beta_7) & \text{for } t \geq \beta_6 + .5\beta_7 \end{cases}$$

$$P(z) = \int_{-\infty}^{z} \frac{1}{\sqrt{2\pi}} e^{(-q^2/2)} dq$$

Before fitting, a priori values for the coefficients are calculated from a linearly-filtered return. A set of standard deviations is assigned to these a priori values indicating how well each coefficient could be approximated from the filtered return. The digitized waveform consisting of digitized "gates" are also weighted in the solution to try to put the heaviest emphasis on fitting to the ramp location(s) which defines the retracking correction. The function coefficients are then solved for using the unfiltered digitized return by iterating until the parameters defining the ramp positions, Beta(3) and Beta(6), converge to within two percent. After the 3rd iteration some of the standard deviations on the parameters are decreased to stop the procedure from either diverging or going into a limit-cycle situation. This process usually works, but it is using a linear solution to a non-linear problem and sometimes unexpected results occur. When the functional fit process fails, the retracking correction is calculated using the threshold-type algorithm discussed above for near-specular returns.

2.3.3. Calibration Issues

2.3.3.1.TOPEX

Calibration of the TOPEX satellite altimeter is an ongoing concern. This PATHFINDER project uses the most recent calibration adjustments. We have applied corrections based on internal calibration-mode estimates of the altimeter range drift, provided by the Wallops Flight Center PATHFINDER team members. We have also corrected for the error in the oscillator drift that was discovered in July 1996.

In addition we have applied a correction for drift in the measured backscatter coefficient, σ_0, although this affects estimates of sea-surface height only through the EM-bias correction. The σ_0 adjustment (up through T/P cycle 40) is described by Callahan, Hancock, and Hayne (1994).

2.3.3.2.POSEIDON

POSEIDON range measurements are corrected on-board the spacecraft with an internal calibration. As of now, there is no reason to suspect a drift in the Poseidon altimeter aboard the T/P satellite after the internal calibration has been applied by CNES. This statement rests primarily on comparisons of the Poseidon-based sea-surface elevations with elevations measured at oceanic tide gauges.

2.3.3.3.ERS-1

There is a known bias in the ERS-1 altimeter of between 40 and 45 cm. The altimeter appears to be ranging short, so derived sea-surface heights are too high by this amount. The bias has been estimated from observations at the ERS-1 Venice calibration site (Francis et al., 1993) and from crossover comparisons with T/P altimetry (Le Traon et al., 1995; Brian Beckley, unpublished results, 1997). Our colinear dataset has NOT been corrected for this bias, but the grid data product is adjusted (see Table 7).

2.3.3.4.Geosat

There are several corrections that have been applied to the Pathfinder Geosat products to compensate for some long-term drift-like errors. Two of them, a calibration-mode adjustment to the altimeter and a drift adjustment to the oscillator, are shown in Figure 6.

The `cal-mode' (or calibration-mode) drift can be detected by the altimeter itself when a synthetic pulse is passed through part of the internal electronics (see MacArthur et al., 1987). The result of such processing is shown in the top portion of the figure. In addition to a very small long-term drift, there are anomalous `humps' that occur near the beginning of each calendar year and are correlated to on-board spacecraft temperatures. We have evidence that these humps are real, because they tend to ``straighten out" estimates of global mean sea-level computed from the altimetry. Therefore, we have applied this correction to the Pathfinder products in the form shown.

The Geosat clock or oscillator was found to drift about 3 parts per billion per year. This was noticed during the original processing of the altimetry, and it was `corrected' midway through the mission by a shift of 10 parts per billion. We have unapplied this shift and then corrected for a constant drift of roughly 2 mm per year in sea level. The bottom portion of Figure 6 shows the correction that we have applied, including the allowance for the shift during October 1987.

• *Figure 6   Variation in Geosat clock oscillation.*
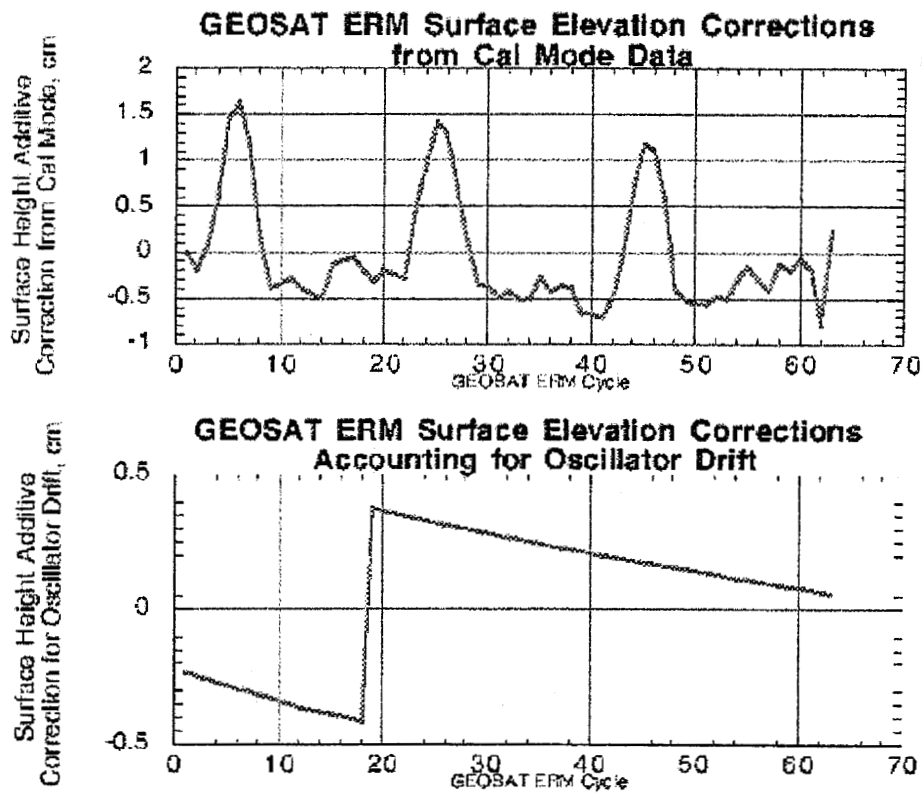
2.3.3.5. Seasat

Height calibration values from Seasat are not reported herein. Upon completion of a formal estimate of the sea state bias by Gaspar, geocenter offsets relative to T/P will be computed and reported in Table 7 at http://neptune.gsfc.nasa.gov/oceans.html.

2.4. Atmospheric Range Refraction Corrections

2.4.1. Dry-Atmosphere Range Refraction Correction

The dry atmospheric range correction is designed to correct the observed altimeter sea-surface elevations for propagation delay caused by refraction through the dry component of the atmosphere. It requires an estimate of the barometric surface pressure at the satellite nadir point. Given this pressure P in mbar, the dry-atmosphere correction is approximated by (Saastamoinen, 1972)

- *Eq. 5   Dry Atmosphere Correction = -2.277*P*[1.0 + 0.0026*cos(q)] mm*

Where, q is twice the latitude. This approximation assumes that the dry atmosphere obeys the perfect gas law and that it is in hydrostatic equilibrium. The small second term shown in brackets accounts for the variation in surface gravity owing to the Earth's ellipsoidal shape.

The pressure data used here are extracted from the operational model of the European Centre for Medium-Range Weather Forecasting, which is updated every 12 hours (except for T/P where a special 6-hour product has been used).

- *Figure 7   Distribution and size of the dry atmosphere range refraction correction (mm), during the ERS-1 mission Phase C cycle 2, i.e. during the 35 day interval beginning on 19 May 1992. The mean correction during this period was 2305 mm, with a standard deviation of 26 mm.*


```
2210    2245    2280    2315    2350
```

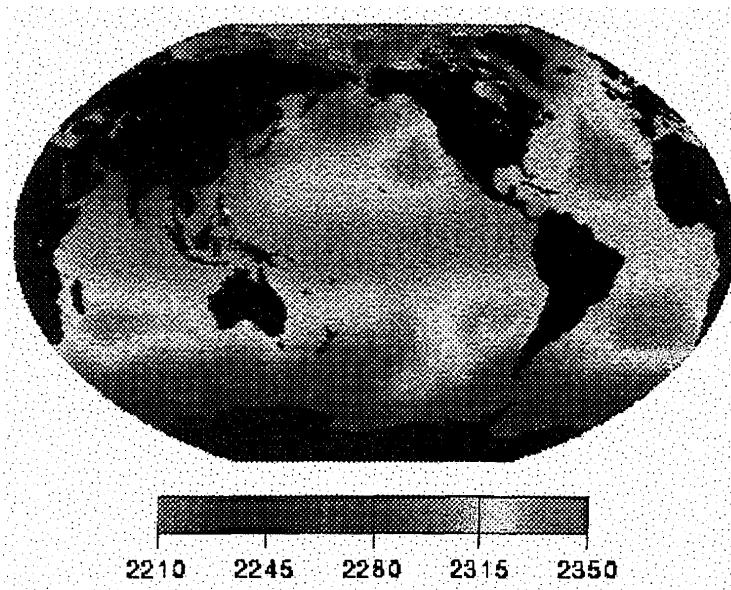### 2.4.2. Wet-Troposphere Range Refraction Correction

The wet troposphere range correction is designed to correct the observed altimeter sea surface elevations for the propagation delay caused by refraction through atmospheric water vapor and cloud liquid water. Although it is smaller than the corresponding dry atmosphere range correction, the wet correction is more complex, with possibly rapid variations in both time and space. This correction can vary from just a few millimeters in dry, cold air to more than 40 cm in hot, wet air.

T/P: The correction is based on the measurements of the T/P on-board microwave radiometer. This is a 3-channel (operating at 18, 21, and 37 Gigahertz), nadir-viewing instrument, which provides nearly direct measurements of the wet-troposphere range refraction correction by monitoring the strong water-vapor absorption line centered at 22.235 GHz. The radiometer and its corresponding data-processing algorithms are described in a series a three papers published in the IEEE TGRS (Ruf et al., 1995; Janssen et al., 1995; Keihm et al., 1995). The radiometer was calibrated in flight during the first few months of the T/P mission; this calibration work is described by Ruf et al. (1994). Further work concerning the validation of this instrument includes Stum (1994) and Keihm and Ruf (1995). The accuracy of this calibration is now being called into question, in 1997, because of a suspected 1-2 mm per year drift in the height measurement that may be caused by the radiometer drift.

ERS-1: The correction is based on the measurements of the on-board microwave radiometer. This is a 2-channel (operating at 23.8 and 36.5 Gigahertz), nadir-viewing instrument. The radiometer and its corresponding data processing algorithms and initial performance are described by Bernard et al (1993).

Geosat: Unlike some altimeter missions, this mission did not include an on-board microwave radiometer that would normally monitor the nadir atmospheric water content. For Geosat wet-troposphere corrections, we must rely on other sources. Earlier versions of Geosat datasets have used climatological analyses from Nimbus-7 SMMR data, operational products from the Fleet Numerical Oceanography Center, and data from the TIROS Operational Vertical Sounder (TOVS) and from the SSM/I instrument on the DMSP satellite. The last two are based on the work of Emery et al. (1990).

For this Pathfinder product, we use the computed `precipitable water' field that has been produced in the recent Reanalysis Project of the NOAA National Centers for Environmental Prediction. For a description of this project, see Kalnay et al. (1996). The columnar water vapor has been converted to a troposphere range refraction correction by use of the high-order algorithm of Liu et al. (1990); this algorithm takes account of the variability of atmospheric equivalent temperature.

22

• *Figure 8   Distribution and size of the wet atmosphere range refraction correction (mm), during cycle 30 of the T/P mission, i.e. during the 10 day interval starting 7 July 1993. The mean correction during this time was 156mm, the maximum 454mm and the minimum 0mm.*
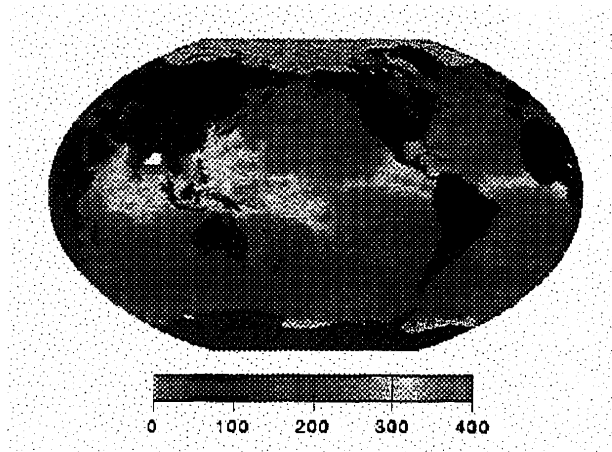
2.4.3.   Ionosphere Range Refraction Correction

The ionosphere range refraction correction to the altimeter data compensates for the propagation delay in the travel time caused by the presence of free electrons in the atmosphere, primarily the ionosphere.

2.4.3.1.TOPEX

For the first time, the TOPEX altimeter allows for a direct measurement of this effect, rather than relying on numerical models as in previous satellite-altimeter missions. This is done through the use of a dual-frequency altimeter, one frequency in the C band (5.3 GHz) and the other in the traditional Ku band (13.6 GHz). Because the ionosphere refraction delay is, to a good approximation, inversely proportional to frequency squared, the two altimeter height measurements yield a direct first-order correction for the time delay. Further discussions of the TOPEX ionosphere measurements can be found in Imel (1994).

The raw ionosphere correction in TOPEX measurements is slightly noisy and requires smoothing before it is applied to the altimeter range measurements. This is done by a local Gaussian convolution filter, with a width of 20 one-second altimeter measurements. Figure 9 shows a long section of altimetry (beginning approximately at MJD 49062.8) with the raw ionospheric corrections and their smoothed counterpart in red. The ionosphere's characteristic bimodal enhancement about the equatorial electrojet, its dependence on local time, and its dependence on solar declination are all apparent in Figure 10, which displays the mean ionosphere correction during the first two months of 1994 at four different local times. As anticipated, the maximum correction occurs at mid-day. Also, since the sun is in the southern hemisphere during January and February, the ionosphere correction is enhanced in that hemisphere.

The ionospheric range delay computed from the TOPEX data has an expected accuracy of 0.5 cm.

- *Figure 9   Section of T/P altimetry (beginning at approximately MJD 49062.8) with the raw ionospheric corrections and their smoothed counterparts in red.*
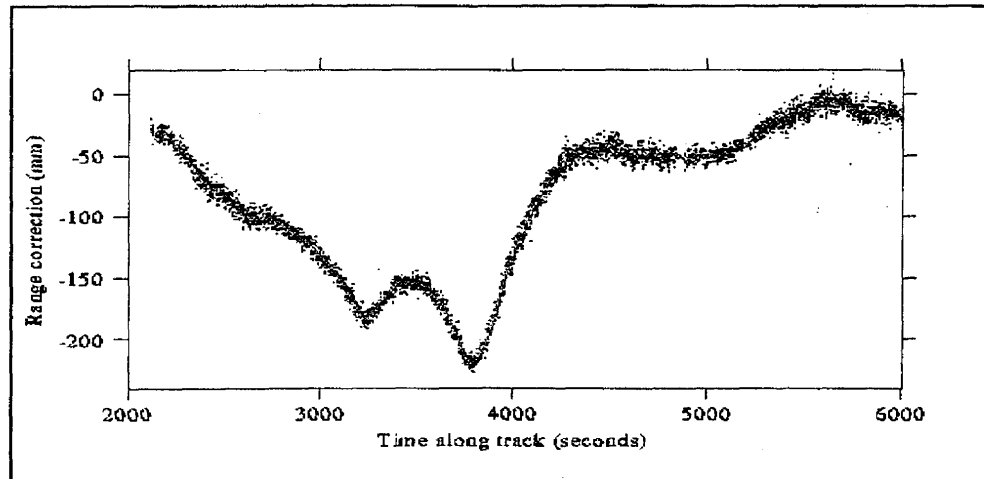
• *Figure 10   The mean ionosphere correction (mm) during the first two months of 1994 at four different local times. Mean local times of measurements given above each plot.*

• *00:00 - 02:00*

• *06:00 - 08:00*

• *12:00 - 14:00*

• *18:00 - 20:00*
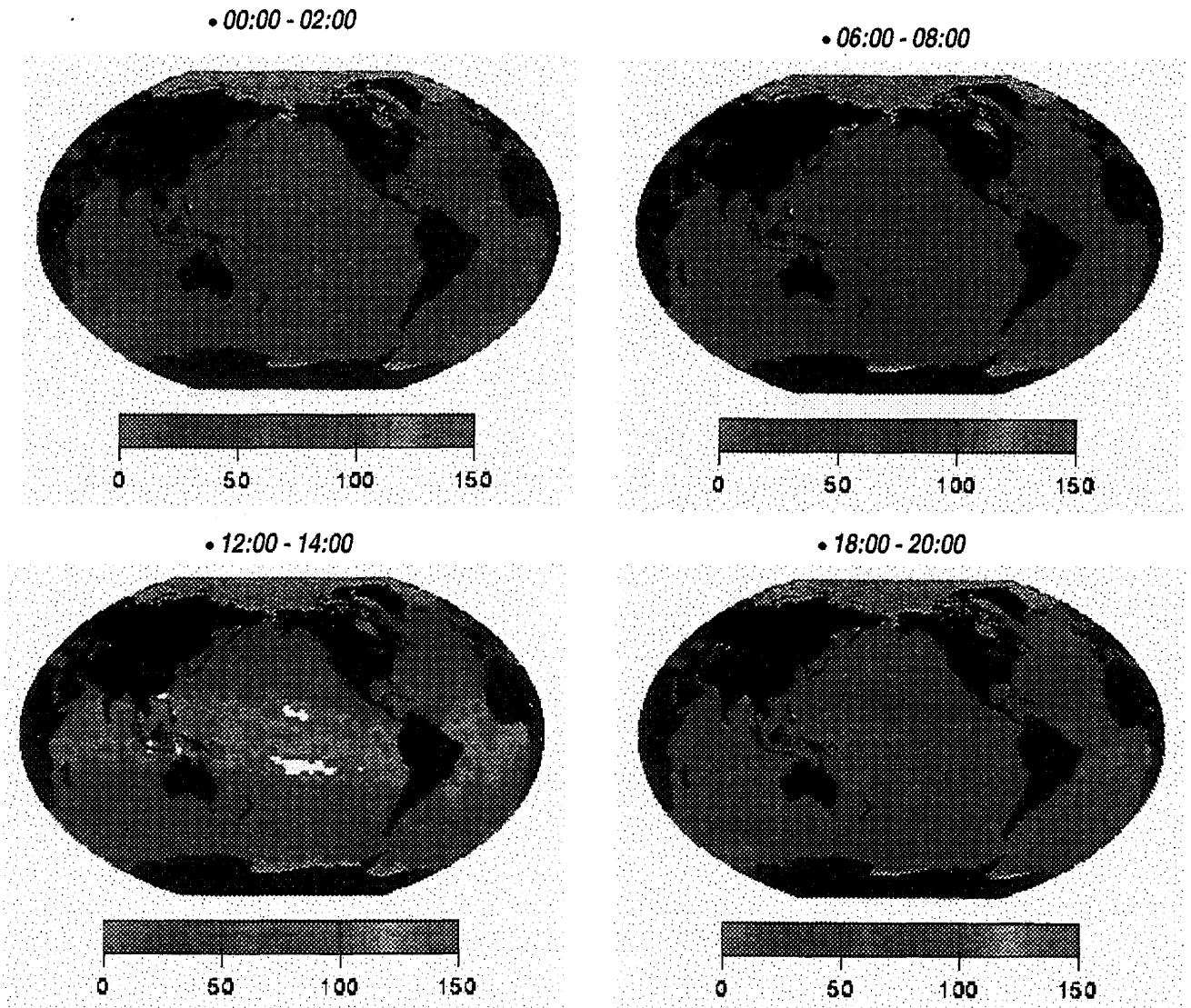
2.4.3.2.POSEIDON

For the Poseidon altimeter, this correction is based on ionospheric measurements made with the DORIS dual frequency receiver aboard the T/P satellite and DORIS beacons at many ground locations. As the DORIS receiver overflies the beacons, the Doppler shift difference in the two frequencies is monitored and then combined with the Bent ionospheric model (Bert and Llewellyn, 1973) to generate a map of the ionosphere corresponding to the appropriate local time.

When the TOPEX altimeter is operational, its dual-frequency ionospheric measurements may be compared to the estimated DORIS measurements. Figure 11 shows an example, based on one series of measurements beginning at approximately MJD 49062.8. The raw unsmoothed TOPEX measurements of ionospheric path correction are compared to the estimated correction for DORIS, shown in blue.

- *Figure 11 The raw unsmoothed TOPEX measurements of ionospheric range refraction are compared to the estimated correction from DORIS model, shown in blue. Beginning at approximately MJD 49062.8*
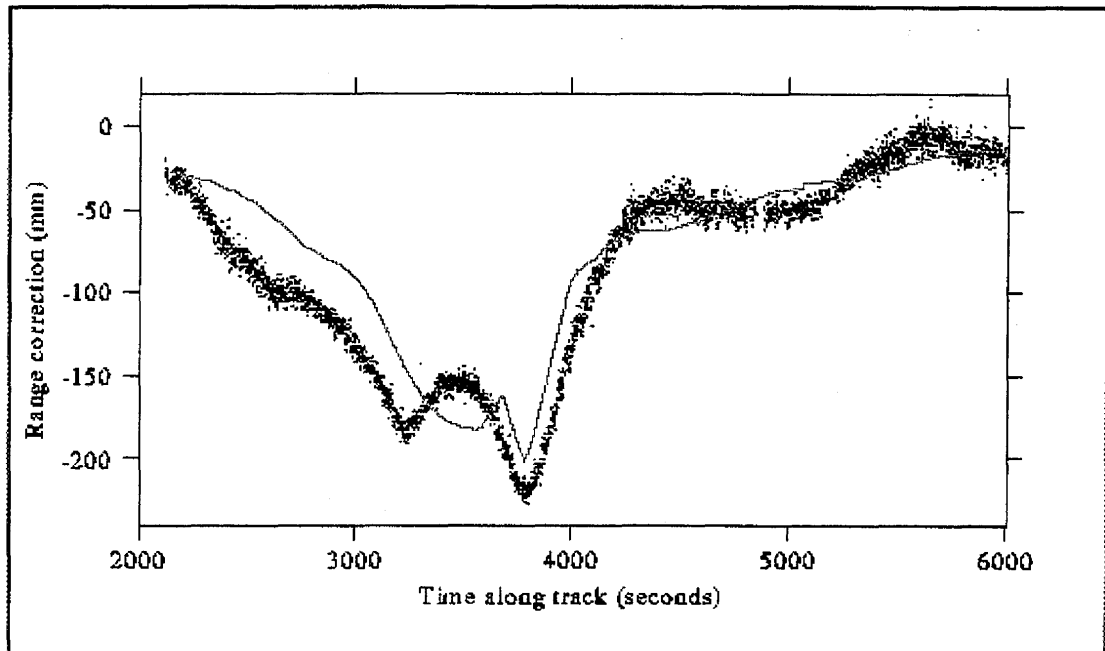
2.4.3.3. Geosat and ERS: IRI95 Ionosphere Correction for Altimeters

When lacking direct altimeter measurements of the ionospheric delay we rely on other data or on models of the ionosphere. For ERS-1, Seasat, and Geosat altimetry, we use the International Reference Ionosphere 1995 (IRI95), specifically Version 13 dated January 1996, in combination with a special ionosphere-effective, solar index. This index is obtained from ionosonde measurements, which during the Geosat time period comprised about 70 globally distributed stations.

The IRI95 model represents a marked improvement over earlier models (Bilitza, 1997, Bilitza et al.,1995). However, by comparing it to actual ionosphere observations made by the TOPEX altimeter, it is easy to find periods when the IRI95 model yields an inaccurate correction for altimetry. Figure 12 is an example. Near the equatorial electrojet, the IRI95 underestimates the required correction by order 10 cm. (Also shown for comparison is the ionosphere correction from the DORIS system, as used for POSEIDON altimetry.) We

emphasize that this plot has been purposely selected as an example of inferior performance by the IRI95 model; it is not typical.

• *Figure 12 Comparison of TOPEX TEC measurement, DORIS ionosphere model and IRI95 models.*

Ionospheric Range Correction
1993 Mar 16 18:00
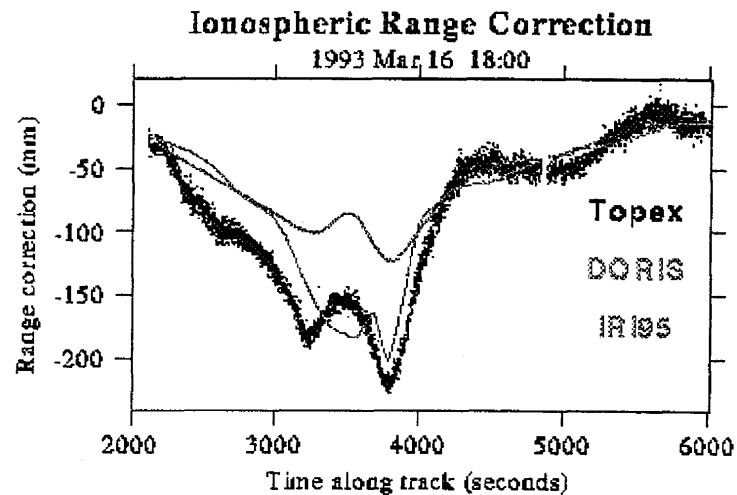
2.5. Geophysical Corrections

2.5.1. Solid-Earth Body Tide Correction

The Earth's body tide is modeled as a purely elastic response to the lunar and solar tidal potentials. The algorithm used here for all satellites is identical to that used for the T/P GDR data, in order to maintain consistency with the ocean-tide models, which by and large depend on T/P data.

The lunar and solar tidal potentials are computed from the semi-numerical expansion of Cartwright and Tayler, described by Cartwright and Edden, (1973), extrapolated linearly to the 1990 epoch. The complete expansion is used, with terms of both second and third degrees in the potential. Only the first term, from the permanent tide, has not been used. By agreement (within the T/P Science Working Group), the permanent tide is included in the geoid model.

The body-tide vertical displacement depends on the adopted h_2 and h_3 Love numbers. For the T/P and Pathfinder projects, the following Love numbers were adopted:

$h_2 = 0.609$ for all terms of degree 2, except
$= 0.52$ for the K_1 tide and its nodal sidelines.
$h_3 = 0.291$ for all terms of degree 3.

These terms are approximately those computed by Wahr (1981), with the exception that Wahr found $h_2 = 0.606$ for long-period tides and a much more complex behavior in the diurnal band surrounding the nearly diurnal free-wobble frequency. Also, all latitude dependence in the Love numbers has been neglected. As noted above, however, we have followed the T/P algorithm for consistency with the ocean tide models

2.5.2. Ocean Tide Correction Version 2.0

The ocean tide removal in the altimeter surface height measurement is the largest of all standard corrections. For example, in an analysis of collinear differences of sea-surface heights, Ray, Koblinsky, and Beckley (1991) found that the ocean tides were responsible for more than 80% of the signal variance.

The Pathfinder ocean tide model for all satellites is actually a combination of many models. The primary deep-ocean model is an updated version of Schrama and Ray (1994). This is version 960104 (hereafter SR960104), but it is nearly identical to version 950308, which was studied extensively by Shum et al. (1997). The model is a long-wavelength adjustment to the FES94.1 hydrodynamic model of Le Provost et al (1994) (this is also the case for Richard Eanes's CSR3.0 model). Cycles 9 to 71 of both TOPEX and POSEIDON data were used in the model development; an adjustment for the JGM-3 ephemerides was done so that the model is consistent with the second-generation orbits available for T/P. Model SR960104 differs from SR950308 only in some slight adjustments toward higher latitudes, which were necessary to extend the model into latitudes above 66°. The model is given on a 0.5° grid.

The SR960104 ocean tide model has 7 primary tidal constituents: O_1, P_1, K_1, N_2, M_2, S_2, and K_2. The Q_1 constituent has been adopted directly from model FES95.2.1 of Le Provost et al. (1994); this Q_1 is an assimilation solution, based on T/P data. In addition to these 8 constituents, 16 minor constituents are accounted for in the tidal-height predictions; these terms are inferred from the major tides by the admittance method (Munk and Cartwright, 1966). Nodal corrections for lunar tides are, of course, incorporated. Finally, the long-period tides are handled similarly to the T/P GDRs: they are assumed to be in equilibrium; the 15 largest spectral lines in the Cartwright and Edden (1973) tables have been used, including the 18.6-year nodal tide but not the permanent tide.

In the polar oceans (latitudes above 66°), including Hudson Bay, the ocean-tide model is FES94.1, although with some slight adjustments near the transition to SR960104 in order to allow for (relatively) smooth corrections without boundary jumps. Therefore, all latitudes overflown by the ERS-1 altimeter have ocean-tide corrections available. However, they should be considered less accurate than latitudes overflown by T/P where the SR960104 model directly incorporates the T/P measurements.

The available global T/P-based tide model is not accurate in shallow seas. In these areas, the tides are spatially complex and the spatial averaging that is necessary to overcome tidal aliasing problems in altimetry cannot be performed

without considerable distortion of the tidal signal. The use of local hydrodynamic models may therefore often be preferable.

The Pathfinder project has begun an effort to supplement the above global tide model with a number of local high-resolution hydrodynamic models for various marginal and inland seas. For the ocean-tide corrections in current use, the list below shows which model has been used in which location.

- Mediterranean Sea: From Canceil, Agelou, and Vincent (JGR, in press). Available on a 0.1° grid.
- Persian Gulf: From Proctor, Flather and Elliott, Continental Shelf Research, 14, 531, 1994. Available on a 5' grid.
- Gulf of Maine: From A. Lambert (Bull d'Infor Mar Terr, 110, 8017, 1991) which is a synthesis of results by Godin ('Cotidal Charts for Canada,' Dept. Fish. Oceans, 1980) and Greenberg (Marine Geodesy, 2, 161, 1979). Includes the lower Bay of Fundy. Given on a 0.25° grid.
- Gulf of St Lawrence: From A. Lambert (Bull d'Infor Mar Terr, 110, 8017, 1991), essentially the same as Godin ('Cotidal Charts for Canada'). Given on a 0.25° grid.

In addition, inland seas as well as the Black Sea and Baltic Sea are assumed to have no tides, which is not strictly true, but no accurate models are currently available. The one body of water with known large tides but with no available (and reasonably accurate) model is the Red Sea.

We are accumulating additional local models for this project, and new versions of our altimeter products will gradually reflect this.

The utility of local models for handling the tide corrections in marginal and shallow seas can be seen from the following experiments. Two-cycle differences of T/P collinear sea-surface heights were processed along three tracks segments(track 101 across the Gulf of Maine and tracks 3 and 54 across the Persian Gulf). The rms of the height differences were tabulated using (a) no tide correction at all (b) the tide correction adopted for the second release of the GDRs (i.e. CSR3.0) and (c) the local models adopted in this project.

• Table 4 Impact of local tide models: RMS of collinear differences (cm).

Track	No tidal correction	GDR model correction	Pathfinder local model correction
101	133	95	18.7
3	39	34	15.3
54	68	75	20.4

The reduced variances resulting from using the local models provides convincing evidence of the value of these models.

• *Figure 13   Geographic distribution of the coverage of the NASA Ocean
Pathfinder Project Ocean Tide Model.*

Schrama-Ray 960104, a long-wavelength adjustment to FES94.1

FES94.1, a hydrodynamic model by Le Provost et al. [1994]

Various local hydrodynamic models
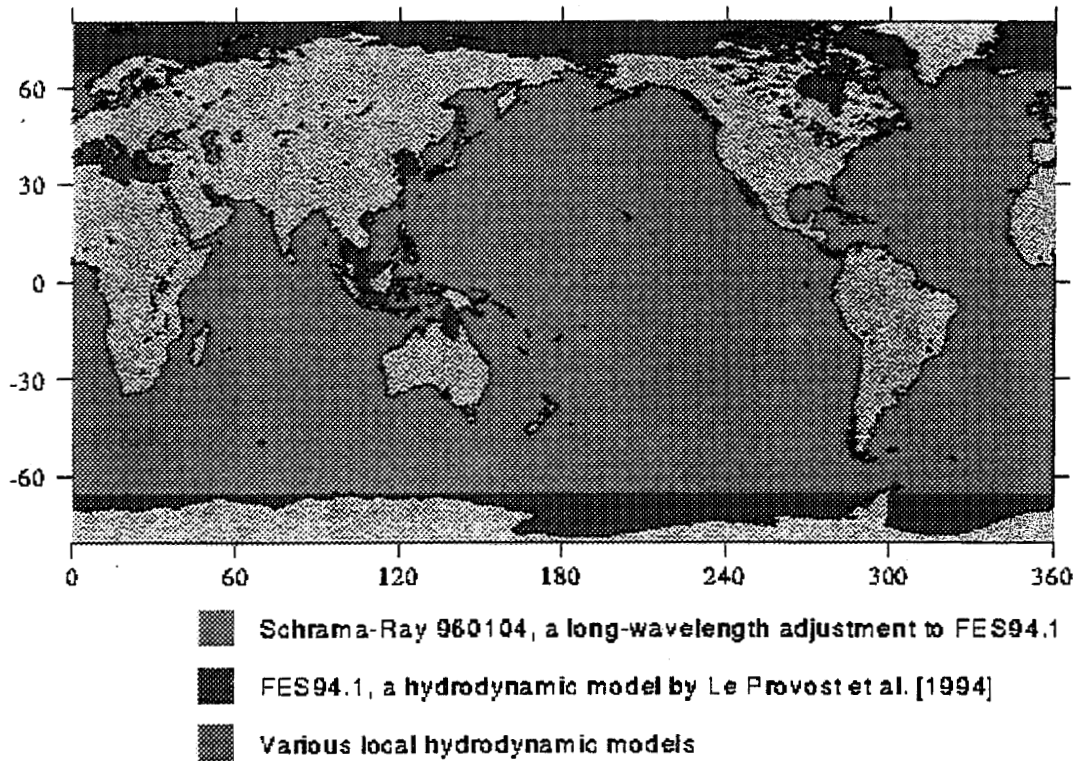
• *Figure 14   Geographic distribution of the M2 ocean tide amplitude (cm)
according to model SR950308. White lines denote cotidal phase lines.*
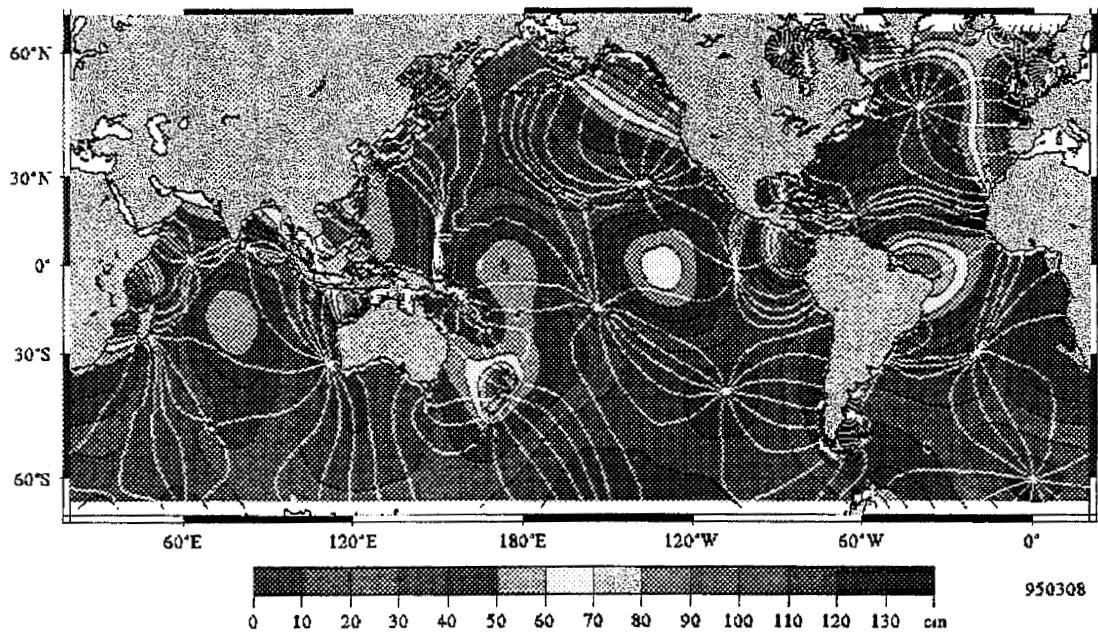
- *Figure 15 Geographic distribution of the Pathfinder Ocean tide model differences with respect to CSR model (cm).*
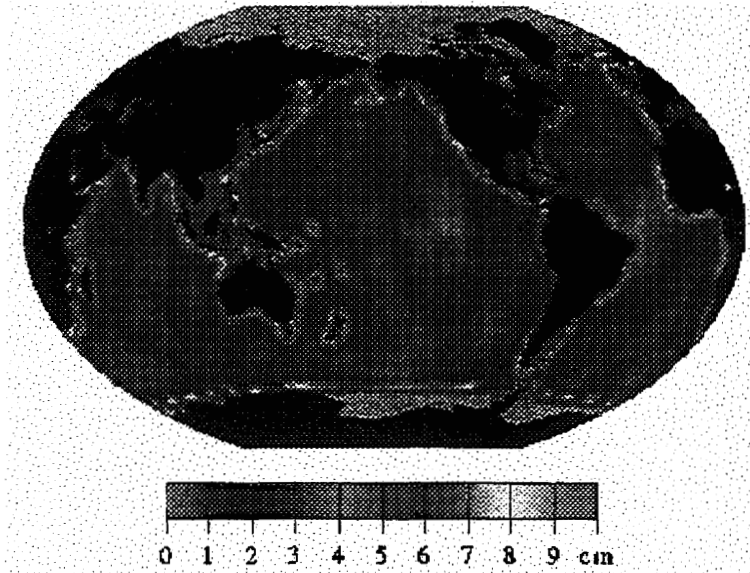
Figure 15 shows the difference in cm between the Pathfinder ocean-tide model and the CSR3.0 model produced by Richard Eanes (University of Texas). The figure gives the maximum difference observed between the two model over a particular day (10 Oct 1995). (The band at the highest latitudes has been purposely increased---see below). These two T/P-based models are clearly very similarly over nearly over nearly all the deep ocean. In shallow and marginal seas, where the tides become larger and spatially complex, there are much larger differences between models.

In the Pathfinder collinear data products, this image has been used for setting the "Suspect Tide Correction" flag bit. Wherever the tide-model differences exceed 5 cm, this bit has been turned on. The latitudes outside T/P's inclination (i.e. those exceeding 66 degrees) require special handling. In those latitudes, both the Pathfinder model and CSR3.0 use the hydrodynamic model (FES94.1) of Le Provost, which is, of course, much less reliable than the T/P-based model. To reflect this, the model differences in these regions have been artificially inflated, and the suspect tide bit is always on.

2.5.3. Load Tide Correction

The load tide describes the local vertical displacement of the solid earth caused by the weight of the overlying ocean tide. The load tide must therefore be consistent with the model used for the ocean tides. The load tide is here modeled as a purely elastic response to ocean loading, using a high-degree expansion in spherical harmonics (to degree and order 360). The response of each degree depends on the loading Love number h'_n ; these have been adopted from the

calculations by Farrell (1972). Further detailed descriptions of this method of computing the load tide can be found in Ray and Sanchez (1989). The amplitude of the M_2 load tide, in millimeters, is shown in Figure 16. The largest amplitudes reach 5 cm off the coast of Brazil. For the diurnal load tides, the largest amplitudes are in the northern Pacific (e.g. the Gulf of Alaska) and off the coast of Antarctica; in these regions the K_1 load tide reaches nearly 3 cm.

• *Figure 16 Geographic distribution of the M_2 amplitude of the ocean load model (mm).*
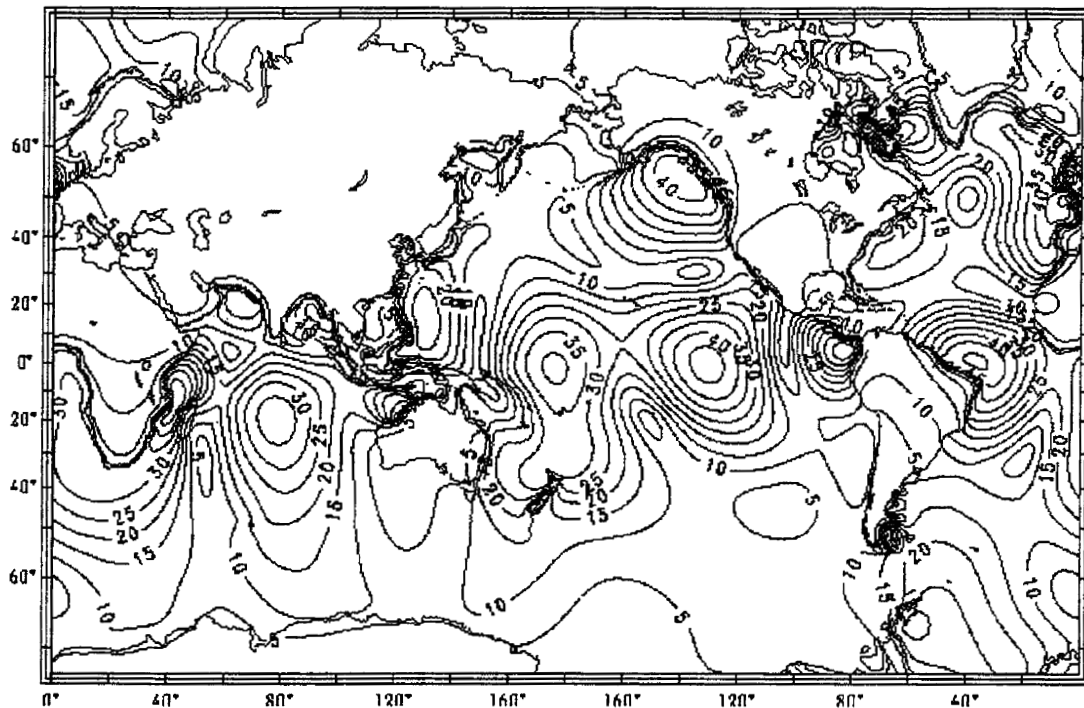
2.5.4. Pole Tide Correction Version 2.0

The pole tide is the response of the ocean (and also of the elastic earth) to variations in the centrifugal force caused by wobbling of the earth's rotation axis. The pole tide has two dominant frequencies: annual and 14-month, the latter being the period of the Chandler Wobble.

The pole tide correction to the altimetry is a geocentric correction, meaning that it includes both the ocean and the solid-earth pole tide. An equilibrium response has been assumed for the ocean. The computed effect is given by Munk and MacDonald, (1960):

• *Eq. 6 Pole Tide elevation = A*sin(2*lat) * [x*cos(lon) + y*sin(lon)]*

Where, x and y denote the position of the pole along the Greenwich and 90°E meridians, respectively. Because the pole position has a non-zero mean, which itself drifts slowly with time, a linear trend is first removed from (x, y). The (x, y) positions of the pole are obtained from the standard 5-day time series of the International Earth Rotation Service, Paris.

The amplitude A = -68.85 mm when (x, y) are expressed in arcsec. However, when the altimeter is overflying an inland sea, not connected to the global ocean, only the solid-earth·pole tide is effective. For that case, A is scaled by the Love number factor h/(1 + k) = 0.47.

• *Figure 17 The (x, y) data of the Pole tide model since 1958, including the linear trend.*
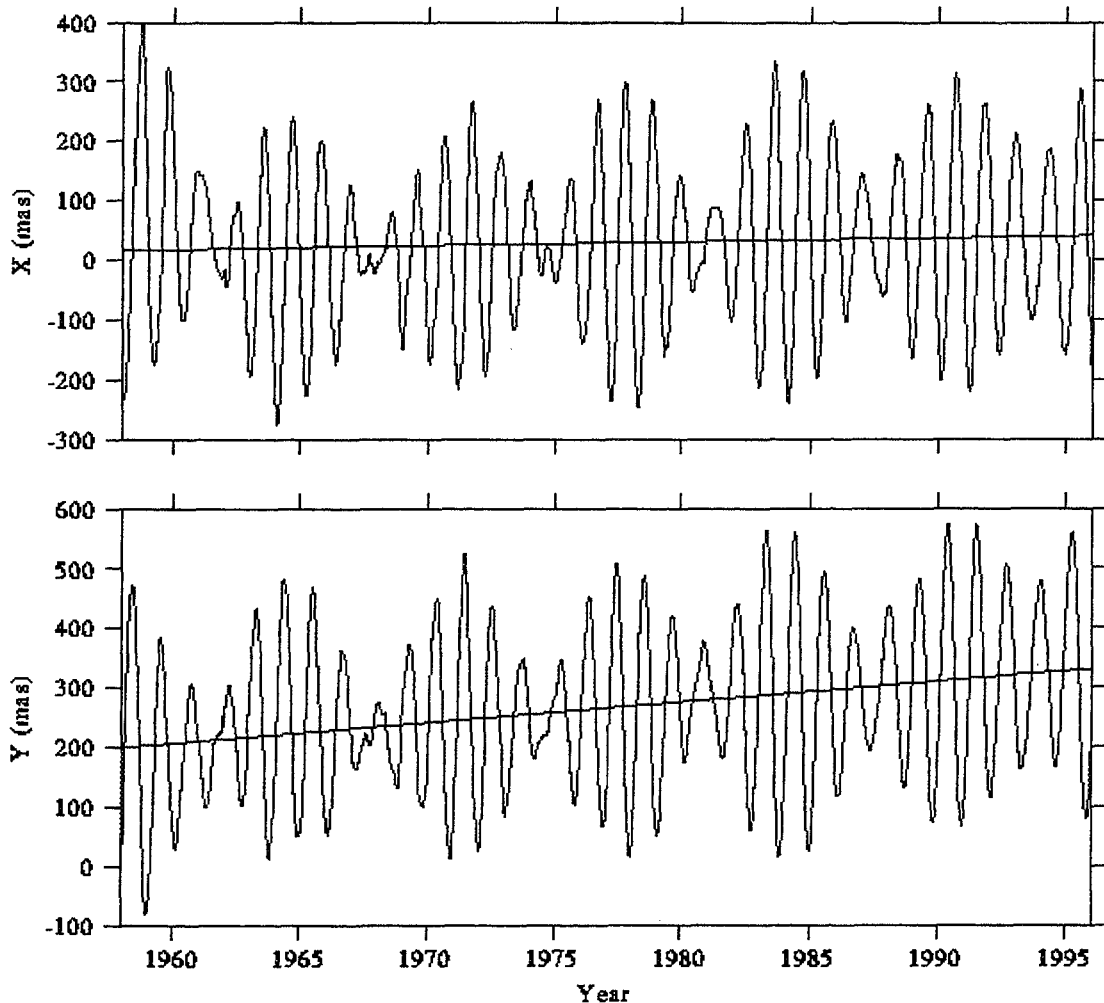
Pole Tide Correction
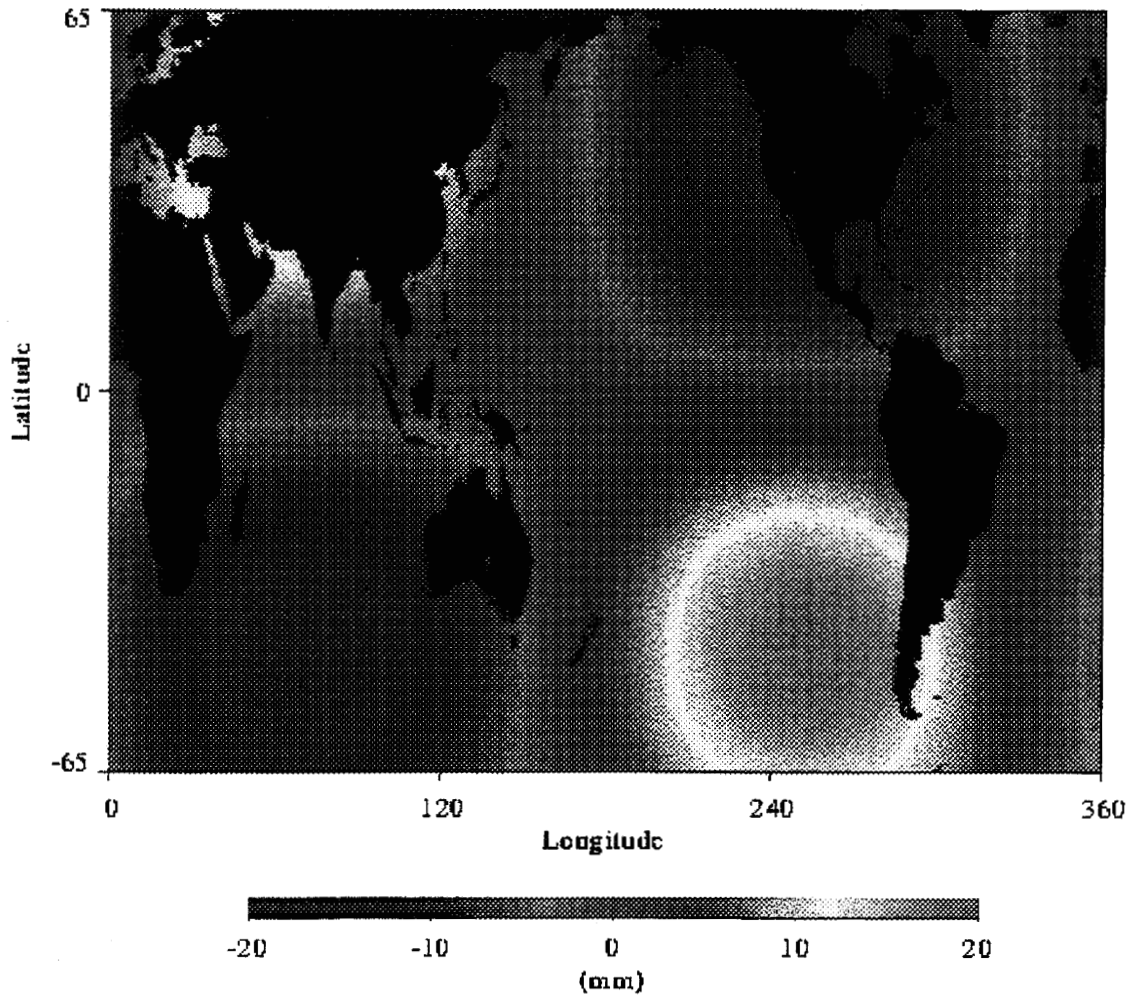
2.5.5. Crosstrack Geoid Correction

Altimeter satellites are maintained in a repeating orbit to facilitate the separation of sea-height variations from the geoid. Perturbations in the satellite orbit result in excursions from the ``exact repeat'' groundtrack. For Geosat this drift caused the groundtrack to vary by more than ±1 km about the nominal repeat path. This misalignment leads to an error in the estimates of sea surface height variations because of the local slope in the geoid (Brenner et al., 1990). High resolution

mean sea surfaces have been constructed from the combined Geosat, ERS-1, and T/P altimeter data sets enabling the computation of accurate geoid slopes normal to the reference repeat orbit. The geoid gradients used in these PATHFINDER products were computed from the mean sea surface CSRMSS95IB, developed at the University of Texas.

Does this correction demonstrably improve the data? An examination of the variances of sea-surface height differences after applying or not applying this correction (in the manner of Ray, Koblinsky, and Beckley, 1991) suggests that the correction is indeed of value. Using data from both Geosat and T/P, we found variance reductions for both satellites of order 1 cm^2.

- *Figure 19   The geographic distribution of the ascending and descending orbit cross track geoid gradient correction (mm) for Geosat, ERM Cycle 27.*
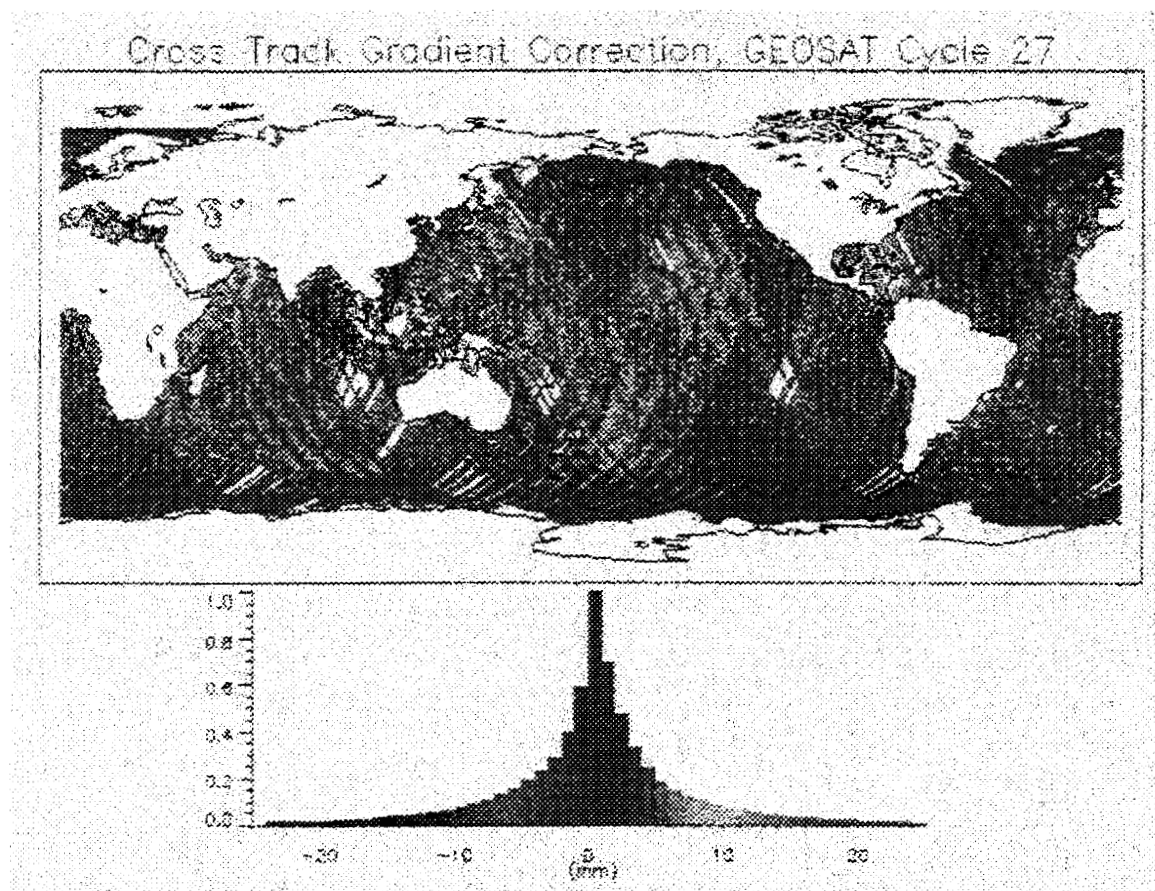
2.5.6. Atmospheric Loading (Inverted Barometer)

Some of the Pathfinder datasets have been adjusted for atmospheric loading. This is useful in many applications when the effects of atmospheric loading are not of interest, for example in the estimation of surface geostrophic currents. This loading 'correction' is done by use of a simple, isostatic, inverted barometer assumption (Gill, 1982):

• *Eq. 7   Inverted Barometer Correction = -9.948 * (P - 1013.3) millimeters*

Where, P is the atmospheric surface pressure in millibars and 1013.3 is the global mean atmospheric pressure. In our data processing, these surface pressures are consistent with the ones used for the dry-troposphere correction. For T/P, Geosat, and ERS-1 the pressures used are the operational products of the European Centre for Medium-range Weather Forecasting (ECMWF). For Seasat, we have used surface pressures from the Fleet Numerical Ocean Center atmospheric model.

• *Figure 20   The geographic distribution of the atmospheric load (mm) determined from the ECMWF surface pressure fields and the inverse barometer response model. This is the mean load during cycle 2 of the ERS-1 Phase C Exact Repeat Mission, i.e. during the 35-day interval starting 19 May 1992.*

-300 -200 -100   0   100 200 300
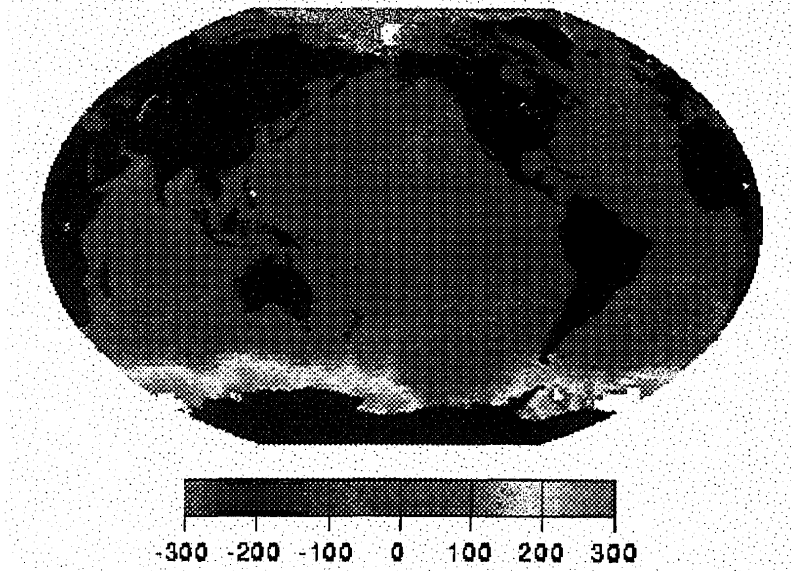
3.1.   Description

The Ocean Altimeter Pathfinder Project began its work by reproducing all GDRs for each mission with revisions based upon the corrections described above. These new GDRs formed a basis for the formation of 'easy-to-use' products. The first product created from these data and distributed to the community was the simplified collinear data set. This data set consists of files containing regularly spaced, spatially-indexed, collinear sea surface heights with respect to a reference mean sea surface. These data were derived from collinear mission data only. For the temporal coverage of the collinear missions see Table 5.

- *Table 5 Collinear data coverage.*

YEAR	Jan	Feb	Mar	Apr	May	June	July	Aug	Sep	Oct	Nov	Dec
78							___[2]	___[2]	___[2]			
79												
80												
81												
82												
83												
84												
85												
86											Geosat	Geosat
87	Geosat	Geosat	Geosat	Geosat	Geosat	Geosat	Geosat	Geosat	Geosat	Geosat	Geosat	Geosat
88	Geosat	Geosat	Geosat	Geosat	Geosat	Geosat	Geosat	Geosat	Geosat	Geosat	Geosat	Geosat
89	___[1]	___[1]	___[1]	___[1]	___[1]	___[1]	___[1]	___[1]	___[1]	___[1]	___[1]	___[1]
90												
91								___[3]	___[3]	___[3]	___[3]	___[3]
92	___[3]	___[3]	___[3]	___[3]	ERS-1	ERS-1	ERS-1	ERS-1	ERS-1 & T/P	ERS-1 & T/P	ERS-1 & T/P	ERS-1 & T/P
93	ERS-1 & T/P	ERS-1 & T/P	ERS-1 & T/P	ERS-1 & T/P	ERS-1 & T/P	ERS-1 & T/P	ERS-1 & T/P	ERS-1 & T/P	ERS-1 & T/P	ERS-1 & T/P	ERS-1 & T/P	ERS-1 & T/P
94	T/P[3]	T/P[3]	T/P[3]	T/P	T/P	T/P	T/P	T/P	T/P	T/P	T/P	T/P
95	T/P	T/P	T/P	ERS-1,2 & T/P	ERS-1,2 & T/P	ERS-1,2 & T/P	ERS-1,2 & T/P	ERS-1,2 & T/P	ERS-1,2 & T/P	ERS-1,2 & T/P	ERS-1,2 & T/P	ERS-1,2 & T/P
96	ERS-1,2 & T/P	ERS-1,2 & T/P	ERS-1,2 & T/P	ERS-1,2 & T/P	ERS-1,2 & T/P	ERS-2 & T/P	ERS-2 & T/P	ERS-2 & T/P	ERS-2 & T/P	ERS-2 & T/P	ERS-2 & T/P	ERS-2 & T/P
97	ERS-2 & T/P	ERS-2 & T/P	ERS-2 & T/P	ERS-2 & T/P	ERS-2 & T/P	ERS-2 & T/P	ERS-2 & T/P	ERS-2 & T/P	ERS-2 & T/P	ERS-2 & T/P	ERS-2 & T/P	ERS-2 & T/P

1 – GEOSAT Data in 1989 not processed because of excessive orbit error

2 – Seasat never in exact repeat orbit

3 – ERS-1 3-day repeat data not processed for pathfinder

Altimeter satellites that are maintained in a repeating orbit facilitate the separation of sea height variations from the geoid. The term 'collinear' refers to sea surface heights for a particular 'exact repeat orbit' mission that have been georeferenced to a specific groundtrack. The collinear data file contains sea surface heights for each orbit cycle at fixed locations thus allowing for the direct analysis of Sea Surface Height (SSH) variability.

The sea surface heights were corrected for all geophysical, media, and instrument effects are given at 1 second intervals (about 7 km, less for T/P) along the reference track using the algorithms described in Section 2. For each satellite files were created that contain:

a) georeference locations;

b) reference mean sea surface height relative to the reference ellipsoid described in Table 3 at each georeferenced location;

c) the time series of corrected sea surface height at each location;

d) a quality control file that contains a flagword for each observation and

e) a file that provides the observation time at index 1 for each revolution.

Software to access all of the files is provided by the project (see below).

3.2. Processing Procedure for Collinear data product

• Obtain, analyze, and apply the latest state-of-the-art corrections and models, consistent across missions, whenever possible.

• Compute improved GDRs.

• Spatially and temporally interpolate to reference ground-track at 1/sec sampling

• Apply editing criteria to extract bad data

• Compute flag data based on quality control criteria

3.3. General Format for Sea Surface Height (SSH) File

The format of the sea surface height file is a sequence of binary records that contain:

Alongtrack Index

Revolution Number

Array of Sea Surface Heights in mm

All the variables are IEEE 2-byte integers. The array length depends on the number of repeat cycles for the particular database version.

• *Table 6 Summary Information of Altimeter Repeat Missions for Ocean Pathfinder Data Sets as of 12/1/97.*

Satellite	No. Days /Repeat Cycle	Revolutions/ Repeat Cycle	Revolution Period in Seconds	Number of Cycles	Span of Data
TOPEX/ POSEIDON	9.92	127	6745	154	92/09/23 - 96/11/28
ERS-1 Phase C	35.00	501	6038	18	92/04/14 - 93/12/20
Geosat (ERM)	17.05	244	6038	62	86/11/08 - 89/09/30

3.4 Dataset File Names and Descriptions

ssh.dat   File containing the sea surface height residuals (mm) with along track index and revolution number

ssh_noib.dat File containing the sea surface height residuals (mm) with along track index and revolution number. Sea surface heights DO NOT have the inverted barometer correction applied

reforb.dat   File containing geodetic North latitude and East longitude in microdegrees of georeferenced locations

mss.dat   CSR mean sea surface (CSRMSS95IB) interpolated to the indexed georeferenced locations (cm)

flagword.dat Data quality flagword for each observation based on certain criteria.

time.dat   Observation time at index 1 for each revolution. All times are in terms of Modified Julian Dates.

directry.dat Directory of direct-access record numbers referenced by revolution and alongtrack index .

Please note that a revolution is defined as the ground track between consecutive ascending equator crossings. The SSH array contains sea surface heights referenced to the University of Texas Center for Space Research (CSR) mean sea surface (CSRMSS95IB). The mean sea surface was computed from the combined Geosat, ERS1 and T/P altimeter data sets. The Geosat and ERS1 data were globally and simultaneously crossover-adjusted with respect to TOPEX/POSEIDON.

Note: It was discovered in 1996 that a miscalculated instrument correction was applied to the TOPEX range measurement resulting in an ~13 cm bias. Therefore, the mean sea surface is elevated 13 cm more than it should be with respect to the reference ellipsoid.

3.5. Calculated Offsets between Missions

Mission offsets were computed by solving for Δr, Δx, Δy, and Δz from crossover residuals with respect to a T/P 1993 mean annual profile. Annual mean profiles were computed for Geosat and ERS-1 and crossed into T/P.
i.e. :

    1993 ERS-1 mean profile x T/P 1993 mean profile
    1987 Geosat mean profile x T/P 1993 mean profile

Table 7 Offsets (cm) from crossover residuals relative to TOPEX/POSEIDON.

Satellite	Δr	Δx	Δy	Δz
Geosat	12.4	7.9	3.3	1.8
ERS-1	-43.5	-2.5	-2.5	-1.5

In order to correct the collinear data for these offsets the following formula should be used:

• *Eq. 8 Corrected SSH = SSH + (Δr+Δx*cos(λ)*cos(ϕ)+ Δy*cos(λ)*sin(ϕ)+ Δz*sin(λ))*

Where, ϕ = East longitude, λ= North latitude

The mean sea surface is provided so that sea surface height can be referenced to the TOPEX standard reference ellipsoid, if desired, see Table 3.

3.6. Updates to Collinear Data Set

3.6.1. TOPEX/POSEIDON

TOPEX/POSEIDON Version 2.0 Updates from Version 1.0:
Revised Feb. 19, 1997: Version 2.0
NASA/GSFC Pathfinder TOPEX/POSEIDON Georeferenced Altimetry
Heritage: PODAAC GDR5.0 for TOPEX / PODAAC MGDR for POSEIDON

A secular trend for the Earth's mean pole position has been removed before computing the pole tide. Data over inland seas have been restored. (The exception is the Red Sea, for which reliable tide corrections are lacking.) Ocean tide quality flag bit (see flag documentation). Sea surface height file contains cycles 1 - 154, with the exception of Poseidon cycles 138 and 150.

Sea surface heights were computed with JGM3 orbits. The precise orbital ephemerides for T/P are identical to those used in the second version of the T/P GDRs, as computed by the Space Geodesy Branch at NASA/GSFC. These ephemerides are computed for nominal 10-day arc segments, corresponding to the groundtrack repeat period of the satellite. They are based on force models derived from the JGM-3 earth gravity model, a T/P-based ocean-tide model, a sophisticated `box-wing' satellite model for drag and radiation forces, and on laser and doppler tracking data. Nerem et al. (1993) and Tapley et al. (1994a) describe earlier versions of the orbits. Those papers give many further details on the ephemeris calculations. The present version of the orbits is described by

Marshall et al. (1995), who examine in detail the error budget while presenting strong evidence for a radial orbit accuracy of about 3 cm rms.

Each record contains an array of sea surface heights for the 154 ten day repeat cycles at a single location defined by a revolution number and along track index:

• *Table 8 TOPEX/POSEIDON Parameter File Record Description.*

Variable	Format	Word Size in Bytes
Along Track Index	I*2	2
Revolution Number	I*2	2
Sea Surface Residual Height Array (mm)	I*2	308

Editing was performed on the data based on these criteria. A flagword for each sea surface residual height was set based on certain tests.

3.6.2. ERS-1 Version 2.0 Updates from Version 1.0:

Revised Feb. 19, 1997: Version 2.0
NASA/GSFC Pathfinder ERS-1 Phase C Georeferenced Altimetry Heritage:
   CERSAT OPR 3.0

A secular trend for the Earth's mean pole position has been removed before computing the pole tide. Data over inland seas have been restored. (The exception is the Red Sea, for which reliable tide corrections are lacking.) Major update: Sea surface height is based on Delft DGM-E04 orbits with 1.7 ms time tag bias applied. (see Section 2). Ocean tide flag bit (see flag documentation).

• *Table 9 ERS-1 Parameter File Record Description.*

Variable	Format	Word Size in Bytes
Along Track Index	I*2	2
Revolution Number	I*2	2
Sea Surface Residual Height Array (mm)	I*2	36

Editing was performed on the data based on these criteria. A flagword for each sea surface residual height was set based on certain tests.

3.6.3. Geosat Version 2.0 Updates from Version 1.0:

Revised Feb. 19, 1997: Version 2.0
NASA/GSFC Pathfinder Geosat ERM (Exact Repeat Mission) Georeferenced Altimetry
Heritage: NOAA/NODC GEMT2-Based GDR (with many improvements, including JGM-3 orbits).

A secular trend for the Earth's mean pole position has been removed before computing the pole tide. Data over inland seas have been restored. (The exception is the Red Sea, for which reliable tide corrections are lacking.) Wet tropospheric correction based on NCEP reanalysis model (PWAT). (AMS Bull.77#3,3/96.) (see Section 2). Sea state bias correction. (Gaspar, 1996) (see Section 2) Ocean tide quality flag bit (see flag documentation)

- *Table 10 Geosat Parameter File Record Description.*

Variable	Format	Word Size in Bytes
Along Track Index	I*2	2
Revolution Number	I*2	2
Sea Surface Residual Height Array (mm)	I*2	124

Editing was performed on the data based on these criteria. A flagword for each sea surface residual height was set based on certain tests.

3.7. Validation

The validation of the colinear products are summarized in Table 11 (RMS companion). This validation is fully described in Report #2: Validation Handbook.

- *Table 11 Global Statistics of Sea Surface Height Variations Computed from Collinear Altimetry Compared to Tide Gauge Measurements.*

	# of Stations	Mean RMS (cm)	Mean Correlation
T/P	76	6.77	0.71
ERS-1 Phase C	78	6.47	0.70
Geosat ERM	58	8.55	0.62

4.1. Description

A time series of gridded monthly sea surface height variations with respect to a 1993 mean reference has been generated from all available altimeter observations provided by Seasat, Geosat, ERS-1, and T/P. The grids are created from height anomalies of cross over or collinear data relative to a mean reference set of collinear ground tracks. The time period for these grids is described in Table 12.

• *Table 12 Summary of Monthly Coverage of Grids between 1978 and 1997.*

Year	Jan	Feb	Mar	Apr	May	June	July	Aug	Sep	Oct	Nov	Dec
78							Seasat	Seasat	Seasat			
79												
80												
81												
82												
83												
84												
85				Geosat	Geosat	Geosat	Geosat	Geosat	Geosat	Geosat	Geosat	Geosat
86	Geosat	Geosat	Geosat	Geosat	Geosat	Geosat	Geosat	Geosat	Geosat	Geosat	Geosat	Geosat
87	Geosat	Geosat	Geosat	Geosat	Geosat	Geosat	Geosat	Geosat	Geosat	Geosat	Geosat	Geosat
88	Geosat	Geosat	Geosat	Geosat	Geosat	Geosat	Geosat	Geosat	Geosat	Geosat	Geosat	Geosat
89	——1	——1	——1	——1	——1	——1	——1	——1	——1	——1	——1	——1
90												
91								——2	——2	——2	——2	——2
92	——2	——2	——2	——2	ERS-1	ERS-1	ERS-1	ERS-1	ERS-1	ERS-1 & T/P	ERS-1 & T/P	ERS-1 & T/P
93	ERS-1 & T/P	ERS-1 & T/P	ERS-1 & T/P	ERS-1 & T/P	ERS-1 & T/P	ERS-1 & T/P	ERS-1 & T/P	ERS-1 & T/P	ERS-1 & T/P	ERS-1 & T/P	ERS-1 & T/P	ERS-1 & T/P
94	ERS-1 & T/P	ERS-1 & T/P	ERS-1 & T/P	ERS-1 & T/P	ERS-1 & T/P	ERS-1 & T/P	ERS-1 & T/P	ERS-1 & T/P	ERS-1 & T/P	ERS-1 & T/P	ERS-1 & T/P	ERS-1 & T/P
95	ERS-1 & T/P	ERS-1 & T/P	ERS-1 & T/P	ERS-1,2 & T/P	ERS-1,2 & T/P	ERS-1,2 & T/P	ERS-1,2 & T/P	ERS-1,2 & T/P	ERS-1,2 & T/P	ERS-1,2 & T/P	ERS-1,2 & T/P	ERS-1,2 & T/P
96	ERS-1,2 & T/P	ERS-1,2 & T/P	ERS-1,2 & T/P	ERS-1,2 & T/P	ERS-1,2 & T/P	ERS-2 & T/P	ERS-2 & T/P	ERS-2 & T/P	ERS-2 & T/P	ERS-2 & T/P	ERS-2 & T/P	ERS-2 & T/P
97	ERS-2 & T/P	ERS-2 & T/P	ERS-2 & T/P	ERS-2 & T/P	ERS-2 & T/P	ERS-2 & T/P	ERS-2 & T/P	ERS-2 & T/P	ERS-2 & T/P	ERS-2 & T/P	ERS-2 & T/P	ERS-2 & T/P

1 = Geosat Data in 1989 not processed because of excessive orbit

2 – ERS-1 3-day repeat data not processed for pathfinder

4.2. Processing Procedure for Grid Data Product

•   Obtain, analyze, and apply the latest state-of-the-art corrections and models, consistent across missions, whenever possible.

•   Compute improved GDRs.

- Spatially and temporally interpolate to reference ground-track at 1/sec sampling.

- Apply editing criteria to extract bad data.

- Compute mean reference surface from mean T/P and ERS data sets.

- Compute crossover anomalies for non-ERS or T/P data sets.

- Adjust cross over or collinear anomalies into mean surface.

- Compute grid from anomalies within a given month.

4.3. Algorithm

4.3.1. Mean Reference Surface

The mean reference surface was computed from merged ERS-1 and T/P annual mean heights along ground-tracks for 1993 by adjusting the 35-day ERS-1 mean profile for 1993 into the T/P geodetic frame. The ERS-1 Phase C altimetry was first updated with Delft DGM-E04 JGM3 based orbits and a number of improved geophysical and altimeter range corrections (see Section 2). A mean profile is then computed at each geo-referenced location employing standard edit procedures, including a minimum cycle requirement to avoid seasonal aliasing. Adjustment of the ERS-1 mean profile with respect to the T/P mean profile was performed by crossover minimization within 30° zonal bands modeled by a simple tilt and bias. Crossover analysis of the adjusted ERS-1 mean profile with the T/P mean resulted in a residual rms of less than 3 cm. The " blending " of ERS-1 and T/P mean profiles generates a dense ground-track providing a statistical robust sample of crossover and collinear sea surface height residuals (see Figure 21).

- *Figure 21 Coverage of blended ERS-1 and T/P groundtracks that form reference surface for grids.*

T/P_____   ERS-1 _____
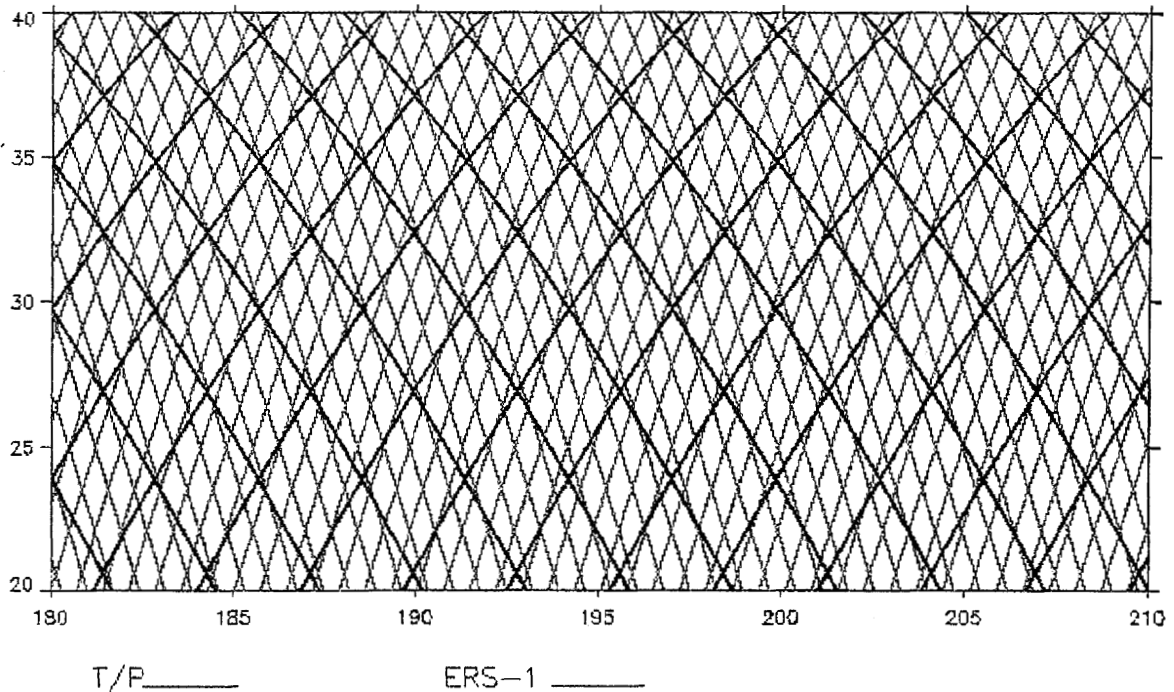
4.3.2. Adjustment Procedure

Significant improvements have been made to the orbit computation based on the JGM3 gravity field for Seasat, Geosat, and ERS missions. However, the orbits have not reached the accuracy of the T/P altimeter mission. Therefore, sea surface height variations computed from Seasat, Geosat, and ERS crossover or collinear residuals with respect to the 1993 reference have been adjusted to remove systematic orbit errors and geocentric offsets. These errors are modeled with a 1 cycle per revolution sinusoid and bias term from the simultaneous crossover minimization of single and dual crossovers to the T/P mean profile.

Reduction of systematic orbit errors employing crossover minimization techniques has a long heritage (e.g., Rapp, 1977; Tai, 1988, 1994; Hwang, 1989; Yi, 1995). It is well known that the orbit error has dominant power at one cycle per revolution (cpr) with secondary peaks at 2 cpr and 3 cpr (Rosborough and Tapley, 1987; Engelis, 1988; Chelton and Schlax, 1993). A low degree polynomial or Fourier series have been used to model the orbit error. An important aspect in using these kinds of error models is that improper use of the error model could remove ocean variability (Tai, 1989; Wagner and Tai, 1994). In order to minimize the loss of ocean dynamics, the polynomial expansion or Fourier series of the lowest possible degree and order have to be chosen. In our study the sinusoidal error model is chosen for one revolution of the altimeter data:

(1) $r(t) = a + b \cos \omega t + c \sin \omega t$

45

where $\omega = 2\pi/T$ is the one cpr for the nodal period of the altimeter mission, a, b and c and are the estimated coefficients for a single revolution. This error model has an along-track wavelength of 40,000 km, thus any effect on the ocean variability has to be at signals with wavelengths of 40,000 km or longer.

The residual sea surface at the single-crossover point (single altimeter mission) is:

$$(2) \quad \Delta h_{ij} = r(t_i) - r(t_j) + \delta^*(t_i, t_j)$$

where t_i, t_j are the times of the ascending and descending arcs at the crossover point; $\delta(t_i, t_j)$ is the time varying sea surface height and error of the environmental corrections at the crossover point. Assuming the TOPEX/POSEIDON mean profile is free of orbit error, the residual sea surface height at the dual crossover point (dual altimeter missions) is:

$$(3) \quad \Delta h_{ij} = r(t_i) + \delta^*(t_i, t_j)$$

Where $\delta^*(t_i, t_j)$ is the sea surface height variation at the crossover point respect to the TOPEX/POSEIDON mean profile and the error of the environmental corrections in both altimeter missions.

Equation (2) and (3) form two observation equations, and the parameters a, b and c for each revolution are estimated through the standard least squares adjustment.

The crossover adjustment procedure has been applied to the Seasat, ERS-1 phase C and Geosat missions. The following table gives the RMS values of the residual sea surface height at the crossover point before and after adjustment.

Table 13 RMS values of the residual sea surface height at the crossover points before and after the adjustment (meters).

		Single Satellite				Dual Satellites		
		Number	Before Adj.	After Adj.		Number	Before Adj.	After Adj.
Seasat (3days)	Cycle 2	516	0.265	0.137		3797	0.534	0.136
	Cycle 5	521	0.257	0.127		3728	0.509	0.128
	Cycle 8	461	0.329	0.121		3556	0.578	0.139
Seasat (17 day)	Cycle 1	3050	0.523	0.121		9547	0.558	0.134
	Cycle 3	6562	0.312	0.119		14063	0.536	0.135
Geosat ERM	Cycle 21	14231	0.151	0.101		20862	0.197	0.120
	Cycle 30	17218	0.163	0.088		25066	0.212	0.105
	Cycle 45	9736	0.222	0.101		17029	0.226	0.110
Geosat GM	Cycle 14	35976	0.153	0.086		37732	0.181	0.098
	Cycle 19	22255	0.136	0.084		30302	0.181	0.100
	Cycle 25	19081	0.128	0.084		27196	0.171	0.102
ERS-1 (35 day)	Cycle10	32507	0.126	0.093		49441	0.421	0.088
	Cycle 15	28467	0.129	0.097		35839	0.475	0.100
	Cycle 17	27109	0.117	0.093		39075	0.449	0.099

4.3.3. Grid Computation

Monthly grids were derived by estimating at each point P on a 1° X 1° regular grid a weighted average of adjacent (within a 3° radius) cross over or collinear differences with respect to the mean 1993 reference surface. Figure 22 shows typical crossover density of points between Geosat GM and the reference surface in mid-latitude regions. In lieu of using an optimal estimator based on local values of the height covariance for smoothing weights, the data weights were derived using an isotropic Gaussian function depending only on the distance from the calculation point $P(\phi,\lambda)$ to the data point at (ϕ_i,λ_i).

• *Figure 22   Groundtrack coverage with respect to 1993 reference frame from*
a) Geosat Primary Mission groundtracks and b) Geosat Exact Repeat Mission
*ground tracks.*

a) GEOSAT Primary Mission

T/P_____   ERS-1 _____   GEOSAT GM _____

b) GEOSAT Exact Repeat Mission

T/P_____   ERS-1 _____   GEOSAT ERM _____
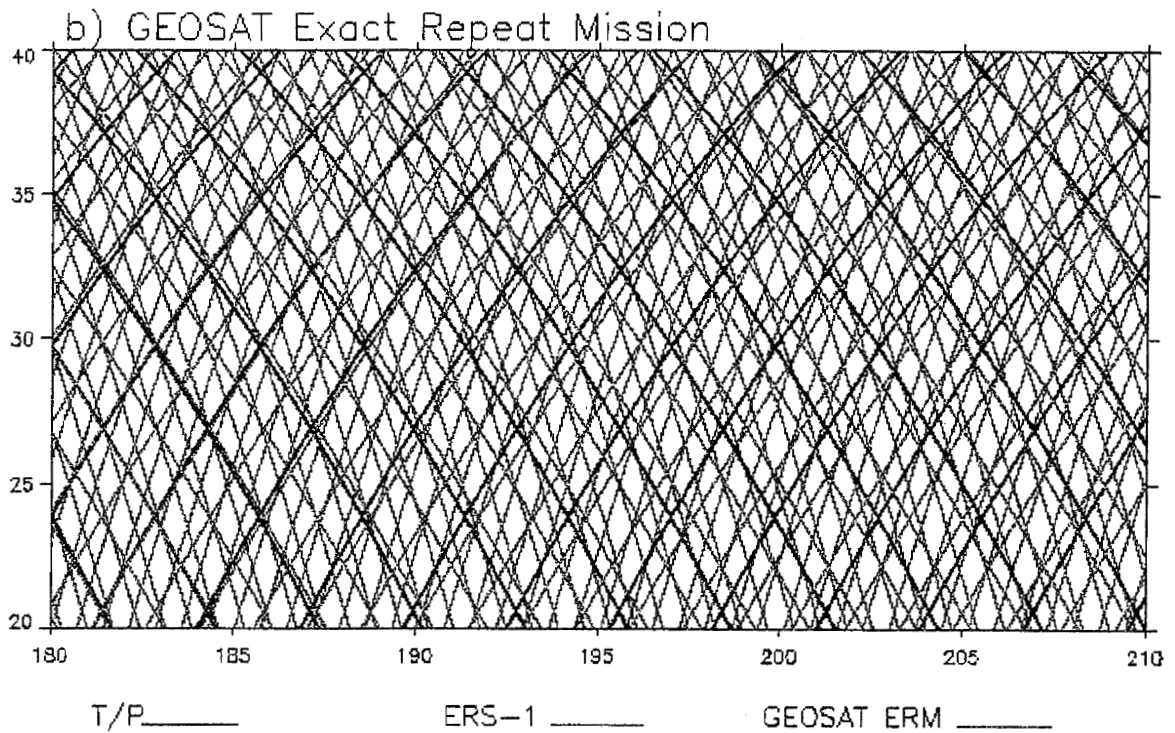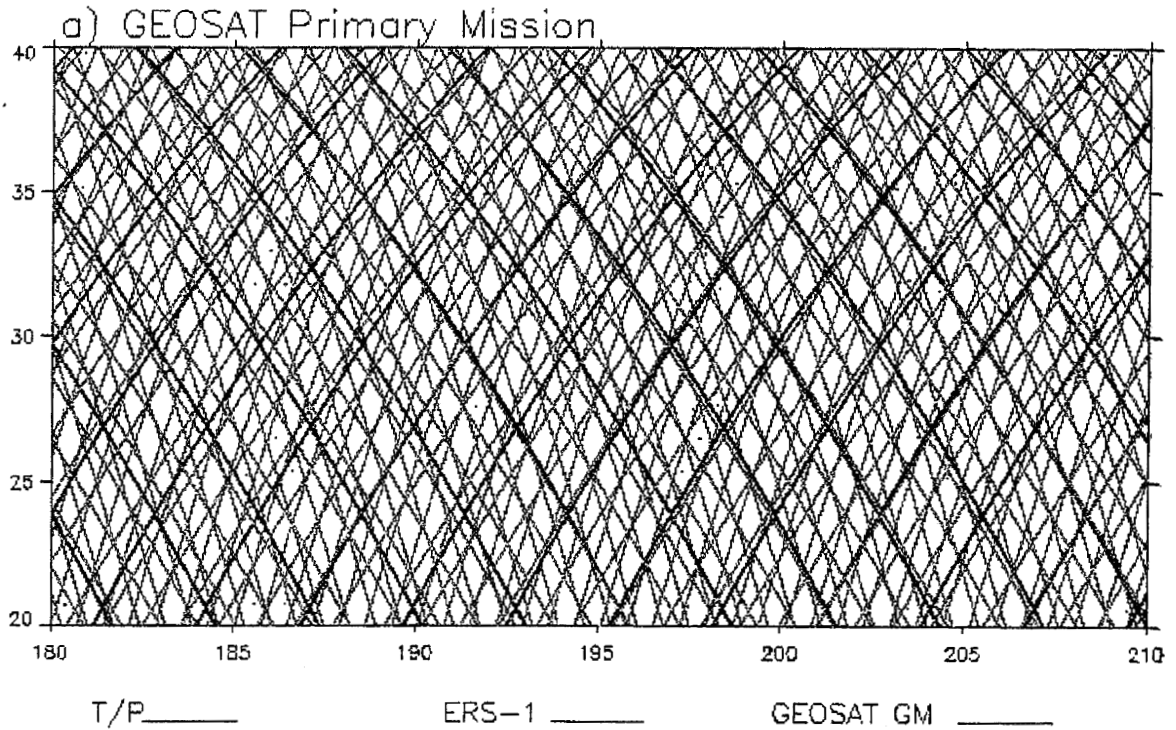
• *Eq. 9 Grid Algorithm*

$$h_p(\varphi, \lambda) = \frac{\sum_{i=1}^{n} w_i \cdot h(\varphi_i, \lambda_i)}{\sum_{i=1}^{n} w_i}$$

Where, $w_i = \exp(-\sigma d^2)$; d = spherical distance between $P(\phi, \lambda)$ and the data points (ϕ_i, λ_i); σ = smoothness parameter defined by the half weight τ, such that: $\exp(-\sigma \tau^2) = 1/2 \rightarrow \sigma = \ln(2)\tau^{-2}$. For our grids, we have selected $\tau = 1°$. Grids of the sea surface height variations are computed using an interpolation procedure to predict a weighted average SSH residual within a defined search radius of the desired grid node. The procedure is fully described in Nerem et al. (1994). Several tests showed that the crossover densities were sufficient to permit a half weight parameter of 1°, and a search radius of 3° (see Figures 23 & 24). The validation of these grids against tide gauge height changes (summarized in Fig. 27) showed that these parameters represent the original data on a global scale. Report #2: Validation Handbook provides complete validation details regarding these grids.

• *Figure 23 Global density of crossover measurements within each grid node from Geosat Primary Mission for a month (November 1985).*
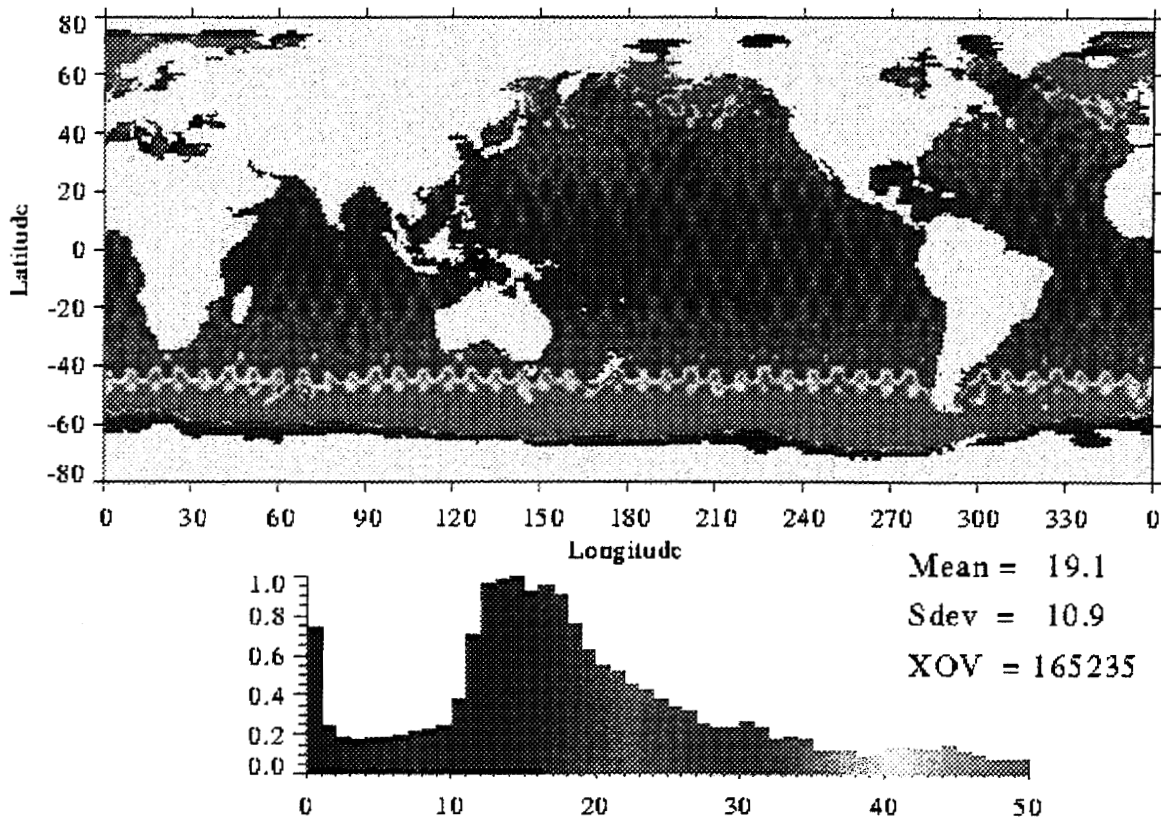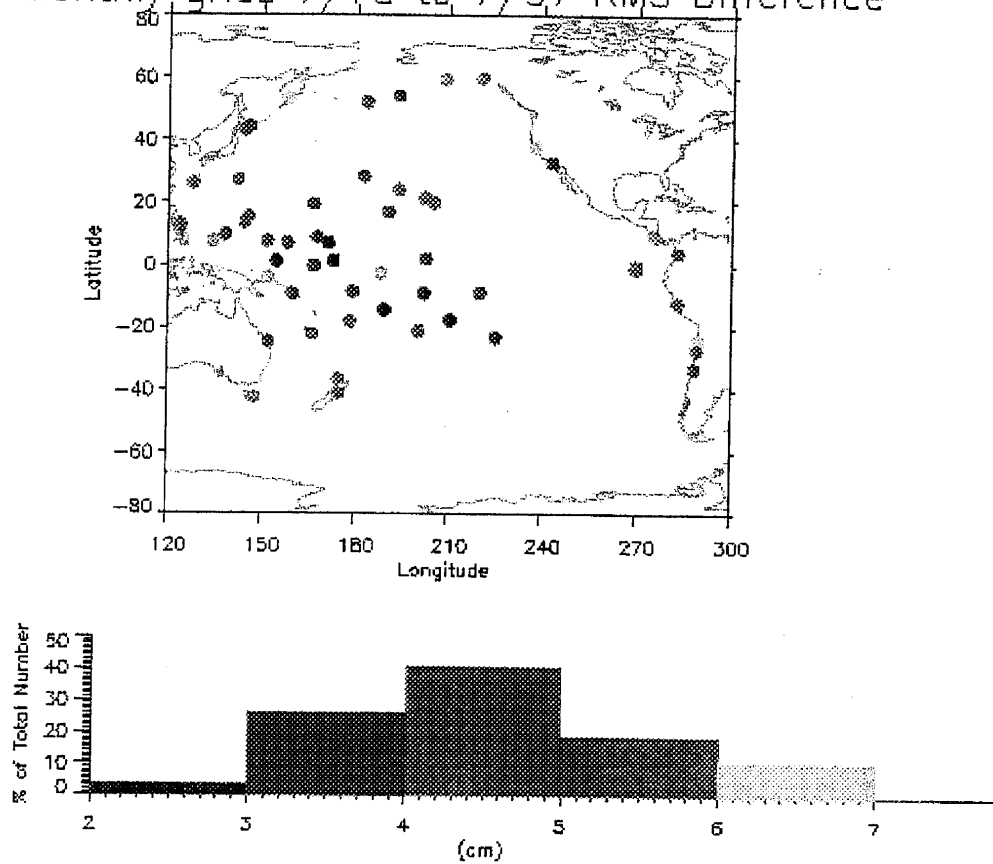
Figure 24 Gridded crossover sea surface height residual for Geosat GM November 1985 with respect to 1993 reference.
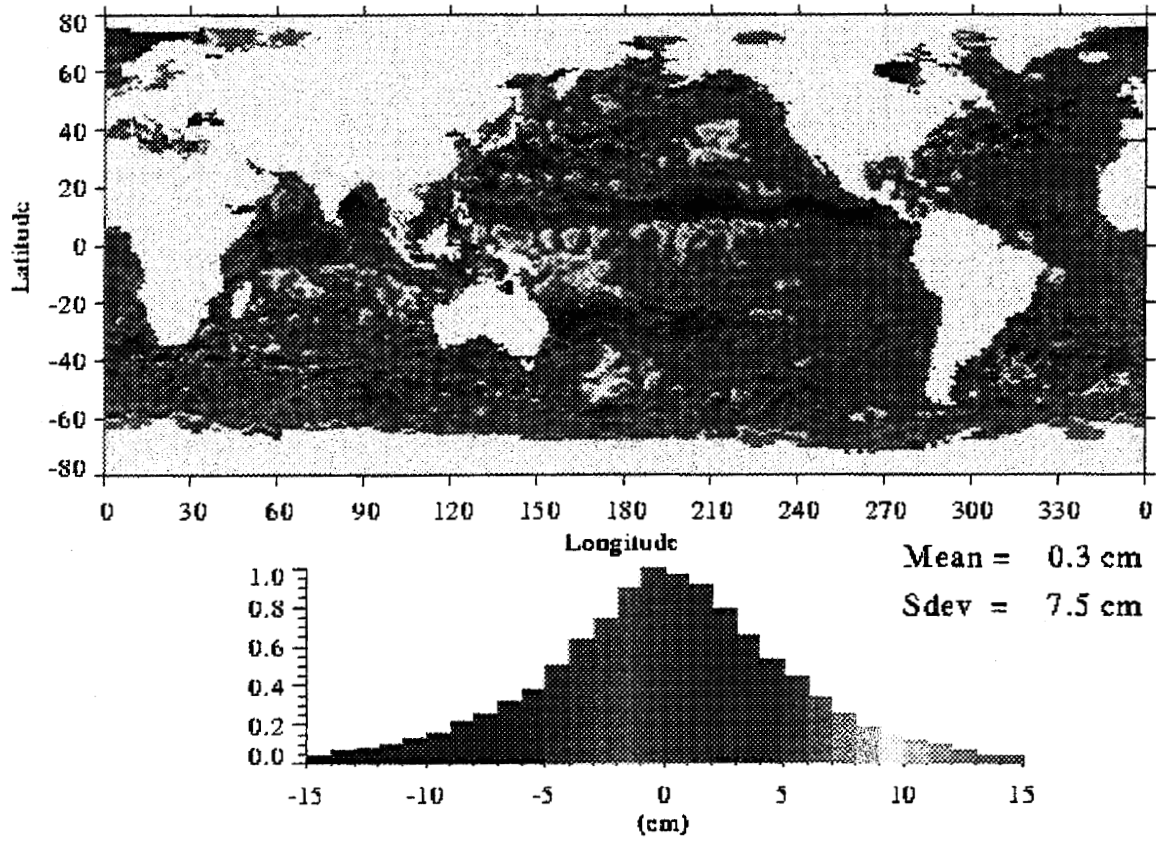
- *Figure 25 Validation of Gridded Altimetry Against Tide Gauge Network. The Mean RMS Difference of the Monthly Grids vs. Tide Gauge is 4.6cm.*

5. References

Bent, R. B., S.K. Llewellyn, "Documentation and Description of the Bent Ionospheric Model," Space and Missiles Organization, Los Angeles, California, AFCRL-TR-73-0657.

Bernard, R., A . Le Cornec, L. Eymard, L. Tabary, "The microwave radiometer aboard ERS-1:Characteristics and performances," IEEE Transactions on Geoscience and Remote Sensing, 31(6), 1186-1198, 1993.

Bilitza, D., International reference ionosphere-status 1995/96. Adv. Space Res., accepted, 1997.

Bilitza, D., C .J. Koblinsky, B. D. Beckley, S. Zia, R. Williamson, "Using IRI for the Computation of Ionospheric Corrections for Altimeter Data Analysis," Adv. Space Res. , Vol. 15, no. 2, pp. 113-119, 1995.

Brenner, A.C., C. J. Koblinsky, B. D. Beckley, "A Preliminary Estimate of Geoid Induced Variations in Repeat Orbit Satellite Observations," Journal of Geophysical Research, Vol. 95, no. C3, pp. 3033-3040, March 15, 1990.

Born, G.H., M.A. Richards, and G.W. Rosborough, "An empirical determination of the effects of sea state bias in SEASAT altimetry," Journal Geophysical Research, 87, 3221, 1982.

Callahan, P.S., D. W. Hancock, and G. S. Hayne, "New sigma-0 calibration for the Topex altimeter," TOPEX/POSEIDON Research News, Issue 3, pp. 28-32, October 1994.

Callahan, P.S., C. S. Morris, and S. V. Hsiao, "Comparison of Topex/Poseidon sigma-0 and significant wave height distributions to Geosat," Journal of Geophysical Research, 99, 25015-25024, 1994.

Callahan, P.S.,TOPEX/POSEIDON NASA GDR Users Handbook, JPL Rep. D-8590, Rev C, Jet Propuls. Lab., Pasadena, Calif., 1993.

Canceil, Agelou, and Vincent (JGR, in press)

Cartwright and Edden, "Corrected Tables of Tidal Harmonics," Geophysical Journal of the Royal Astronomical Society, 33, 253-264, 1973.

Chelton, D.B. and M.G. Schlax, "Spectral characteristics of time-dependent orbit errors in altimeter height measurements," Journal of Geophysical Research, 98, 12579-12600, 1993.

Colombo, O.L., "The dynamics of GPS and the determination of precise ephemeris," Journal of Geophysical Research, 94, 9167-9182, 1989.

Cretaux, J.F., F. Nouel, C. Valorge, P. Janniere, "Introduction of empirical parameters deduced from the Hill's equations for satellite orbit determination," Manuscripta Geod., 19, 135-156, 1994.

Douglas, B.C. and R.W. Agreen, "The Sea State Correction for GEOS 3 and SEASAT Satellite Altimeter Data," Journal of Geophysical Research, 88, 1655-1661, 1983.

Emery, W.J., G.H. Born, D.C. Baldwin, C.L. Norris, "Satellite-derived water vapor corrections for Geosat altimetry," Journal of Geophysical Research, 95, 2953-2964, 1990.

Engelis, T., "On the simultaneous improvement of satellite orbit determination of sea surface topography using altimeter data," Man. Geod., 13, 180-190, 1988.

The ERS-1 System, European Space Agency Publication ESA SP-1146, 1992.

The ERS-2 Spacecraft and Its Payload, ESA Bulletin 83, 1995.

Farrell (Reviews of Geophysics and Space Physics, 10, 761-797, 1972).

Francis, R. et al. (1993) The calibration of the ERS-1 radar altimeter: the Venice calibration campaign. ESA Rep. ER-RP-ESA-RA-0257, 272 pp.

Freilich, M.H., and P. G. Challenor, "A new approach for determining fully empirical altimeter wind speed model functions," Journal of Geophysical Research, 99, 25051-25062, 1994.

Gaspar, P., F Ogor, P-Y Le Traon, O-Z Zanife, "Estimating the sea state bias of the TOPEX and Poseidon altimeters from crossover differences," Journal of Geophysical Research, 99, 24981-24994, 1994.

Gaspar, P., F Ogor and M. Hamdaoui, "Analysis and Estimation of the Geosat Sea State Bias," NASA Ocean Altimeter Pathfinder Project Report #4, 1996.

Geosat: Sea Level from Space, Journal of Geophysical Research, Special Issue, 95, no. C3, October 15, 1990.

The GEOS3 Project, Journal of Geophysical Research, Special Issue, 84, no. B8.

Gill, A., Atmosphere-Ocean Dynamics, Academic, 1982.

Godin ('Cotidal Charts for Canada,' Dept. Fish. Oceans, 1980)

Greenberg (Marine Geodesy, 2, 161, 1979)

Imel, D.A., " Evaluation of the TOPEX/POSEIDON Dual Frequency Ionospheric Correction, "Journal of Geophysical Research, 99, 24895, 1994.

Hwang, C., "High precision gravity anomaly and sea surface height estimation from GEOS-3/Seasat satellite altimeter data," Rep. 399, Dept. of Geodetic Science, The Ohio State University, 1989.

Saastamoinen, J., "Atmospheric correction for the troposphere and stratosphere in radio ranging of satellites," Geophysical Monograph 15, American Geophysical Union, 1972.

Sandwell, D.T.,D.G. Milbert, and B.C. Douglas, "Global nondynamic orbit improvement for altimetric satellites," Journal Geophysical Research, 91, 9447-9451, 1986.

Scharroo, R., P. Visser, and G. Mets, "TOPEX-class orbits for the ERS satellites," submitted for publication in J. Geophys. Res., 1997.

Schrama, E.J.O., and R.D. Ray, "A Preliminary Tidal Analysis of TOPEX/POSEIDON Altimetry," Journal of Geophysical Research, 99, 24799, 1994

Seasat Special Issue I: Geophysical Evolution, Journal of Geophysical Research, 87, no. C5, April 30, 1982.

Shum et al. , "Accuracy Assessment of Recent Ocean Tide Models," Journal of Geophysical Research, 102, 25173-25194, 1997.

Stum, J., "A comparison between TOPEX microwave radiometer, ERS-1 microwave radiometer, and ECMWF derived wet tropospheric corrections," Journal of Geophysical Research, 99, 24927-24939, 1994.

Tai, C.-K., "Accuracy assessment of widely-used orbit error approximations in satellite altimetry," Journal Atmos. Oceanic Tech., 6, 147-150, 1989.

Tai, C.-K., "Geosat crossover analysis in the tropical Pacific. 1. Constrained sinusoidal crossover adjustment," Journal Geophysical Research, 93, 10621-10629, 1988.

Tai, C.-K., and J. Kuhn, "On reducing the large-scale time-dependent errors in satellite altimetry while preserving the ocean signal: orbit and tide error reduction for TOPEX/POSEIDON," NOAA Tech. Mem. NOS EOS 9, 1994.

Tapley, B., J. Ries, G. Davis, R. Eanes, B. Schutz, C. K. Shum, M. Watkins, J. A. Marshall, R. S. Nerem, B. Putney, S. Klosko, S. Luthcke, D. Pavlis, R. Williamson, N. Zelensky, "Precision orbit determination for TOPEX/POSEIDON," J. Geophys. Research, 99, 24383-24404, 1994.

Tapley, B., M .Watkins, J. Ries, G. Davis, R. Eanes, S. Poole, H. Rim, B. Schutz, C. K. Shum, R. S. Nerem, F. Lerch, J. A. Marshall, S. Klosko, N. Pavlis, R. Williamson, "The Joint Gravity Model 3," J. Geophys. Res., 101, 28029-28049, 1996.

TOPEX/Poseidon: Geophysical Evaluation, Journal of Geophysical Research, Special Issue, 99, no. C12, December 15, 1995.

TOPEX/Poseidon: Scientific Results, Journal of Geophysical Research, Special Issue, 100, no. C12, December 15, 1995.

Wagner, C.A., and C.K. Tai, "Degradation of ocean signals in satellite altimetry due to orbit error removal processes," Journal Geophysical Research, 99, 16255-16267, 1994.

Wahr, J.M., "Body Tides on an Elliptical Rotating Elastic and Oceanless Earth," Geophysical Journal of the Royal Astronomical Society, 64, 677-703, 1981

Williamson, R .G., and R. S. Nerem, (abstract), EOS, 75(44), Fall Meeting Suppl., 155, 1994.

Witter, D.L., and D B Chelton, "A Geosat altimeter wind speed algorithm and a method for altimeter wind speed algorithm development," Journal of Geophysical Research, 96, 8853-8860, 1991.

Yi, Y., "Determination of Gridded Mean Sea Surface from TOPEX, ERS-1 and GEOSAT Altimeter Data," Report No. 434, Dept. of Geodetic Sci., The Ohio State University, 1995.